JOURNAL OF PALEONTOLOGY

NEW SKELETAL MATERIAL OF *ANDREWSIPHIUS* AND *KUTCHICETUS*, TWO EOCENE CETACEANS FROM INDIA

J. G. M. THEWISSEN[1] AND SUNIL BAJPAI[2]

[1]Department of Anatomy, Northeastern Ohio Universities College of Medicine, Rootstown 44272, <thewisse@neoucom.edu>; and [2]Department of Earth Sciences, Indian Institute of Technology, Roorkee 247667, <sunilfes@iitr.ernet.in>

J. Paleont., 83(5), 2009, pp. 635–663

0022-3360/09/0083-0635$03.00

NEW SKELETAL MATERIAL OF *ANDREWSIPHIUS* AND *KUTCHICETUS*, TWO EOCENE CETACEANS FROM INDIA

J. G. M. THEWISSEN[1] AND SUNIL BAJPAI[2]

[1]Department of Anatomy, Northeastern Ohio Universities College of Medicine, Rootstown 44272, <thewisse@neoucom.edu>; and [2]Department of Earth Sciences, Indian Institute of Technology, Roorkee 247667, <sunilfes@iitr.ernet.in>

ABSTRACT—The Eocene cetacean genera *Andrewsiphius* and *Kutchicetus* are systematically revised, their anatomy described, and their phylogenetic position analyzed. Each genus contains a single species, *A. sloani* and *K. minimus*, and both are known only from the middle Eocene of the Indian Subcontinent. *Andrewsiphius* and *Kutchicetus* differ in a number of respects, the most important dental difference being that P2, P3, p2, and p3 are double-rooted in *Andrewsiphius* and single-rooted in *Kutchicetus*. Lower molars are separated by diastemata in *Kutchicetus*, but not in *Andrewsiphius*. Postcranially, *Andrewsiphius* has caudal vertebrae that are far more robust than those of *Kutchicetus*.

We propose the new clade Andrewsiphiinae for these two genera, based on their unique characters: the extremely slender jaw, fused mandibular symphysis, narrow palate and rostrum, and lower molars that have a low crown with three cusps lined up rostro-caudally. A phylogenetic analysis indicates that andrewsiphiines are either a subfamily of Remingtonocetidae or an independent branch on the Eocene cetacean lineage. Interpreting conservatively, we classify them as remingtonocetids. Andrewsiphiines have a long, robust, dorso-ventrally flattened tail and short limbs, suggesting that they swam using dorsoventral undulation of the tail.

INTRODUCTION

THE INDIAN subcontinent is commonly held to be the birthplace of cetaceans, and a great variety of Eocene whales is found in northern and central Pakistan and western India. These were reviewed by Thewissen and Bajpai (2001b) and Thewissen and Williams (2002), and important new discoveries on whale origins were added by Gingerich et al. (2001b) and Thewissen et al. (2001, 2007). Among the strangest Indo-Pakistani cetaceans are *Andrewsiphius* and *Kutchicetus*. These whales have long, narrow rostra and mandibles that are much deeper (dorsoventrally) than wide (mediolaterally). Their palate is very narrow, and the mandibular symphysis is fused as far caudal as the molars, making it hard to distinguish an edentulous and fragmentary maxilla from a mandible.

Andrewsiphius was described by Sahni and Mishra (1975) as an early odontocete based on several incomplete and gypsified specimens. Kumar and Sahni (1986) further described the genus and included it in the family Remingtonocetidae, a referral followed by all subsequent authors. Bajpai and Thewissen (1998) described new specimens for *Andrewsiphius*, and Bajpai and Thewissen (2000) reported the discovery of a skeleton for a new genus: *Kutchicetus*. All of the specimens discussed by these authors were found in the Harudi Formation of the District Kutch (also spelled Kachchh) of the State of Gujarat, Western India. Bajpai and Thewissen (2002) and Gingerich et al. (2001a) reported on new fragmentary material from, respectively, the Panandro and Akri Lignite Mines of Kutch, and the Sulaiman Range of central Pakistan.

Our recent field work in Kutch (2002–2008) more than triples the number of fossils known for *Andrewsiphius* and *Kutchicetus*. This allows us to revise the genera systematically, describe the dental anatomy and the postcranial anatomy, and evaluate their place in cetacean evolution.

In India, museum acronyms do not necessarily imply that the specimen is located in the collections of the institution with that acronym, but only that it was initially collected or described by a scientist at that institution. Specimens that were used are catalogued in the following collections: Howard University-Geological Survey of Pakistan, curated by senior author (H-GSP); Lucknow University, Vertebrate Palaeontology Laboratory, Lucknow, India (LUVP); Indian Institute of Technology, Roorkee, curated by Sunil Bajpai (IITR-SB); and Vertebrate Palaeontology Laboratory, Panjab University, Chandigarh, India (VPL). The IITR-SB acronym replaces the RUSB acronym of all previously published and new specimens in this collection. The collection remains located at the same institution, and the specimen numbers remain identical. The change in acronym reflects only the upgrade and name change of the University of Roorkee to the status of Indian Institute of Technology.

SYSTEMATIC PALEONTOLOGY

Order CETACEA Brisson, 1762
Family REMINGTONOCETIDAE Kumar and Sahni, 1986
Subfamily ANDREWSIPHIINAE, new subfamily

Type genus.—*Andrewsiphius* Sahni and Mishra, 1975.

Referred genus.—*Kutchicetus* Bajpai and Thewissen, 2000.

Diagnosis.—Cetaceans with fused mandibular symphysis in adults, which extends to m2 or further posteriorly. Length of p3 less than or equal to p2 and less than or equal to p4. Snout near posterior premolars narrow and high. Palate narrow. Paroccipital process strongly curved and pointing anteriorly, hook-like. Laterally projecting falcate process absent. Eyes near midline, not laterally positioned. Lower molar profile low and elongate, lacking a high anterior trigonid and with no clear distinction between trigonid and talonid. Lower molars with three cusps lined up rostrocaudally, and the second cusp is the highest.

Age and Distribution.—Middle or late Lutetian (middle Eocene) Harudi and Panandhro Formation of Western Gujarat, India, and Lutetian Domanda Formation of central Pakistan. Traditionally, the Harudi Formation has been considered to be middle Eocene (Lutetian) in age (Biswas, 1992). However, some later workers (Singh and Singh, 1991; Rai, 1997) suggested a younger (Bartonian) age for the entire Harudi Formation based on nannofossils recovered near the top of the formation in beds near the *Nummulites obtusus* Zone of Biswas (1992). Gingerich et al. (2001a) also considered

the Harudi Formation Bartonian in age. However, the cetacean-yielding levels of the Harudi Formation occur stratigraphically well below the nannoplankton levels and pertain to an older cycle of sea level change than the one proposed by Gingerich et al. (2001a) since sequence stratigraphic data indicate that there is a hiatus of unknown magnitude between the Harudi and the overlying Fulra Limestone formations (Saravanan, 2007). Consequently, a late Lutetian age for the cetacean-bearing sediments of the Harudi Formation is most consistent with the data. This estimate is further confirmed by a $^{87}Sr/^{86}Sr$ value derived from oyster shell attached to one of the Harudi whale skulls (V. Ravikant, IIT Roorkee, personal commun., February, 2009). These Sr values, seen in conjunction with the recent sequence stratigraphic data on the Harudi Formation (Saravanan, 2007), suggest an age between 41 and 43 m.y.a. Cetaceans from the Panandhro Formation are found in close proximity to lignite deposits at the Panandhro and Akri Lignite Mines. Our previous age inference for these beds (Bajpai and Thewissen, 2002) was based on the traditional inclusion of them in the Naredi Formation, which followed Biswas (1992). Biswas (1992) considered the Naredi Formation to range from late Paleocene to early Eocene in age. While this age estimate may be reasonable at the type section of the formation (where there is neither lignite nor fossil cetaceans), it appears that this is not the case at Panandhro and Akri Lignite Mines. Here, the stratigraphy is more complex and the beds yielding the whales are best included in the Panandhro Formation of Saraswati and Banerjee (1984, preferred here) or the Lakhpat Formation of Mukhopadhyay and Shome (1996). These beds are equivalent in age to the Harudi Formation: middle/late Lutetian. The Domanda Formation of central Pakistan is also Lutetian in age (Gingerich et al., 2001a).

Discussion.—*Andrewsiphius* and *Kutchicetus* are usually thought to be closely related to *Remingtonocetus*, and this interpretation is consistent with some, but not all cladograms in our phylogenetic analysis (see below). There are important differences between *Remingtonocetus* and the andrewsiphiines. In *Remingtonocetus*, p3 is elongate, longer than both p2 and p4. However, p4 is longer than p3 in *Andrewsiphius* and *Kutchicetus*. The lower molars bear three cusps that are lined up anteroposteriorly in several families of Eocene whales. Crown height is much reduced in andrewsiphiines, but the second of these cusps is the tallest, whereas crown height is not reduced and the first cusp is the tallest in *Remingtonocetus*, dorudontids, and basilosaurids.

A fused mandibular symphysis is rare among Eocene cetaceans. Lower jaws of the protocetid *Babiacetus* are fused (Bajpai and Thewissen, 1998), and this condition has been reported in *Remingtonocetus* from Kutch (Kumar and Sahni, 1986). However, most *Remingtonocetus* from Kutch have an unfused symphysis (VPL 1010, IITR-SB 2521, 2812, 2811, 2814), but IITR-SB 2592 and IITR-SB 2938 (a specimen of the closely related *Dalanistes*, molar morphology described by Thewissen and Bajpai, 2001a) have a partially fused symphysis. In most Eocene cetaceans, the mandibular symphysis extends to the anterior premolars, but only in *Andrewsiphius* and *Kutchicetus* does it reach to the molars. The mandibular foramen is large in *Kutchicetus* (IITR-SB 2636) and *Andrewsiphius* (IITR-SB 2650), similar in height to the height of the dentary.

The andrewsiphiine nasal opening is over I3 or C, similar to pakicetids, ambulocetids, and *Remingtonocetus* but unlike dorudontines and basilosaurines. The snout of most Eocene cetaceans, including *Remingtonocetus*, is wider (left plus right mediolaterally) than it is high (dorsoventrally), whereas in *Andrewsiphius* and *Kutchicetus* it is higher than wide, causing the palate to be narrow even at the molars. The M2 and M3 bear a single large cusp, unlike pakicetids, ambulocetids, and some protocetids, but similar to other protocetids and *Remingtonocetus*. The posterior roots of M3 are fused (or, stated differently, consist of a single partly split root), similar to *Remingtonocetus* and some protocetids but unlike pakicetids and ambulocetids.

Andrewsiphius and *Kutchicetus* are cranially very different from *Remingtonocetus*. In *Remingtonocetus*, the orbits are laterally placed under the narrow frontals (see cross-sections of the orbital region in Nummela et al., 2006). In *Andrewsiphius* and *Kutchicetus*, the eyes are perched high on top of the skull (IITR-SB 2791), closer to the median plane, similar to *Ambulocetus* (Nummela et al., 2006). The basicranium of *Remingtonocetus* is dominated by the laterally projecting processes of the basioccipital (often called falcate processes), which articulate laterally with an obliquely placed bulla (Bajpai and Thewissen, 1998). These processes are absent in *Andrewsiphius* and *Kutchicetus*, resulting in tympanics that are located closer to the sagittal plane than in many other Eocene cetaceans. In *Remingtonocetus*, the posterior lumbar vertebrae are more than 10% longer and wider than the anterior caudal vertebrae (UM 3015, Gingerich et al., 1993, specimen identified as *Indocetus*, identification corrected by Gingerich et al., 1995), whereas these vertebrae are similar in length and width in *Kutchicetus*.

Genus ANDREWSIPHIUS Sahni and Mishra, 1975

Protocetus (in part) SAHNI AND MISHRA, 1972, p. 491; 1975, p. 20.

Andrewsiphius SAHNI AND MISHRA, 1975, p. 23; GINGERICH, UL-HAQ, KHAN, AND ZALMOUT, 2001a, p. 288 (in part); BAJPAI AND THEWISSEN, 2002, p. 221 (in part).

Remingtonocetus KUMAR AND SAHNI, 1986, p. 341 (in part).

Type and only species.—*Andrewsiphius sloani* (Sahni and Mishra, 1972).

Diagnosis.—The p2, p3, P2, and P3 always double-rooted. Lower molars not separated by diastemata. Mandible higher than combined left and right mandibles wide near posterior premolars. Lumbar vertebrae similar in length and width to posterior thoracic vertebrae.

Occurrence.—Middle Eocene (Lutetian) of western India and central Pakistan.

Discussion.—Sahni and Mishra (1975) proposed that there are two species of cetaceans with long, narrow and high rostra and mandibles in the Eocene of Kutch: a large and a small species. Their view was correct, but they did not have material of the smaller species. They named the larger species *Andrewsiphius kutchensis*, and this name has been used widely for this taxon (Kumar and Sahni, 1986; Bajpai and Thewissen, 1998). However, restudy of the poorly preserved holotype of *Protocetus sloani* Sahni and Mishra, 1972 (later referred to *Remingtonocetus* by Kumar and Sahni, 1986), indicates that it also represents this taxon. The latter name has priority, as pointed out by Gingerich et al. (2001a).

Sahni and Mishra (1972, 1975) were the first to amass a large collection of cetacean specimens from Kutch. Unfortunately, much of their material was fragmentary and gypsified, and the holotypes they designated far from perfect. However, our much larger and better preserved collection indicates that the alpha-taxonomic designations of Sahni and Mishra were reasonable, and we therefore interpret our specimens conservatively. At this point, the presence of two species of andrewsiphiines can be ascertained, and existing names can

be reasonably applied to these. Since these holotypes are imperfect, we used more nearly complete specimens to infer diagnostic characters. For more incomplete specimens, we used the highly distinct morphological features to identify them as andrewsiphiines (the high and narrow maxilla and mandible), and then standard methods of paleontological inference: inferring occlusal relations between maxillae and mandibles and matching size for specimens for which there was no direct overlap in anatomical elements.

ANDREWSIPHIUS SLOANI (Sahni and Mishra, 1972)

Figures 1, 2.1–2, 2.8–10, 3.1–2, 4.1–2, 5.1–3, 6.4–7, 7, 8.1–4, 8.6, 8.14, 9.9–14, and 10.3–4, 10.11, and 10.14

Protocetus sloani SAHNI AND MISHRA, 1972, p. 491, pl. 97.4–5 (in part); 1975, p. 20 (in part).

Cetacea indet. SAHNI AND MISHRA, 1972, p. 17, pl. 5.5.

Andrewsiphius kutchensis SAHNI AND MISHRA, 1975, p. 23, fig. 3, pl. 5.6. BAJPAI AND THEWISSEN, 1998, p. 221, fig. 6G–H (in part).

Andrewsiphius minor SAHNI AND MISHRA, 1975, p. 25, fig. 5.7.

Remingtonocetus harudiensis KUMAR AND SAHNI, 1986, p. 330, figs. 7C and 10G (in part).

Remingtonocetus sloani KUMAR AND SAHNI, 1986, p. 341, fig. 8k.

Andrewsiphius sloani GINGERICH, UL-HAQ, KHAN, AND ZALMOUT, 2001a, p. 288, fig.14 (in part).

Diagnosis.—*Andrewsiphius* is monospecific, and the specific diagnosis cannot be distinguished from the generic diagnosis.

Description.—This description focuses on jaws and teeth (Figs. 1–7). Other parts of the skull as well as the postcranial skeleton are described below in direct comparison with *Kutchicetus*. Although there are many upper and lower jaws for *Andrewsiphius*, well-preserved crowns of teeth (Fig. 5) are rare. The dental formula is 3.1.4.3/3.1.4.3 (Fig. 11). The I1 through P1 are single-rooted, P2 to M1 are double-rooted (IITR-SB 2031, 2701, 2724, 2742, and 2923). M2 is also double-rooted, but its posterior root is wider than its anterior root (IITR-SB 2907, IITR-SB 7913; Fig. 5) and sometimes partly divided (IITR-SB 3153; similar to *Kutchicetus*, VPL 1007). The M3 has one anterior root and a broad, divided posterior root (IITR-SB 3153; as in *Kutchicetus*, VPL 1007; Fig. 5). Diastemata occur between all teeth from I1 to M1, but not between the molars (IITR-SB 2031 and 2724).

In IITR-SB 2517 (Fig. 1.7), the alveolus for the right I3 is normal, but on the left, parts of a small tooth are visible, probably dI3, which failed to erupt. The upper canine alveolus is only slightly larger in size to I3 and P1. The incisors are relatively large in size compared to the molars. The canine is located on the suture between premaxilla and maxilla (IITR-SB 2517). P1 is single-rooted, P2–4 are double-rooted (IITR-SB 2731, 2742, 2751). Based on their alveoli, upper premolars increase somewhat in length from P2 to P4 (IITR-SB 1724, LUVP 11060). Two specimens have a well-preserved crown for M2 (IITR-SB 3153, length: 21.0 mm; width: 9.4 mm; IITR-SB 2751, length: 19.6 mm, width, 9.2 mm; Fig. 5.1). The crown bears a single large cusp and is thus triangular in labial outline. Crests extend to the anterior and posterior extremity of this cusp, and a small cuspule is located on both the anterior and the posterior crest. The posterior tubercle, probably the metacone, is on a higher position of the crest than the anterior cuspule. The anterior and posterior cingula are distinct, the labial cingulum is weak and not continuous, the lingual cingulum is strong posteriorly and it flares around the lingual root. There are no protocone, parastyle, metastyle, or conules. The base and the posterior side of the crown of M1 is preserved in IITR-SB 2751 (width 5.4 mm). Its morphology is similar to M2, with the small metacone located on the postparacrista. Unlike M2, M1 is not expanded lingually, and there is no trace of a lingual root or a protocone. The M3 is preserved in IITR-SB 2751 (length: 20.1 mm; width: 11.0 mm). It is similar to M2, except that the lingual extension (protocone lobe) is larger than in M2 and that the paracone is placed more caudally on the crown. The presence of a metacone cannot be determined in this tooth because the postparacristid is damaged.

Although most specimens of *Andrewsiphius* lack teeth, alveolar sizes provide some useful insights into dental variation. The ranges in alveolar length are 17–27 mm for M1 (n = 7), 20–22 mm for M2 (n = 9), and 19–33 mm for M3 (n = 11). Large ranges are caused by a few outlying specimens that appear within the normal range of variation for the species in other respects.

In the lower dentition, there are diastemata between all teeth from i1 to m1, but there are no diastemata between the lower molars (IITR-SB 2648 and 2723). The i1 through p1 are single-rooted; the p2–m3 are double-rooted (LUVP 11060, IITR-SB 2526, and 2648; Fig. 2.10).

The i1 is smaller than i2 and i3, judging from its alveolus (Fig. 2.5). The p3 (IITR-SB 2723) is triangular in labial view. Its length is 22 mm. The p4 (IITR-SB 2723: length: 24 mm, width: 10 mm; Fig. 5.3) bears one high cusp from which crests extend anterior and posterior to the tooth's base. The posterior crest is somewhat crenulated. The p4 has a triangular outline in lateral view. There are weak lingual and buccal cingula. The m1 (IITR-SB 2723; Fig. 5.3) is a low tooth with three cusps arranged anteroposteriorly and crests extending over these cusps from anterior to posterior cingulum. The anterior cusp and posterior cusp are similar in height; the middle cusp is higher, and a cingulum surrounds the tooth (length: 26 mm, width: 7 mm). We consider the middle cusp the protoconid, the anterior cusp the paraconid, and the posterior cusp the hypoconid. However, given the highly unusual morphology of this tooth, these identifications remain tentative.

The mandible is narrow and deep (Figs. 2.1–2, 3.1–2), with left and right jaw firmly fused (synostosis), making the anterior mandible resemble the anterior palate. Along the inferior side of the mandible, the mandibular symphysis extends posteriorly to a variable degree. The shortest mandibular symphysis ends below the contact between m1 and m2 (IITR-SB 2723), and it reaches further in other specimens (LUVP 11002, 11132; exact extent in these cannot be determined because of breakage). In other specimens, the mandibular symphysis terminates under m3 (IITR-SB 2526) or even beyond m3 (LUVP 11060, IITR-SB 2650). On the alveolar rim, the mandibular symphysis ends at a more anterior level. Here, the mandibular symphysis ends and the left and right mandibles diverge between p4 and m1 (LUVP 11002), or further posteriorly (LUVP 11132, 11060). Laterally the mandibles are more or less flat, and inferiorly they form a sharp crest, best shown in cross-section (Fig. 3.1–2). This differs strongly from *Remingtonocetus*, where the cross-section is oval and the lower edge not sharp but rounded (e.g., IITR-SB 2592, 3018; Thewissen and Bajpai, 1998). In the protocetid *Babiacetus* (IITR-SB 2512, Bajpai and Thewissen, 1998) the lateral and inferior sides of the mandible are also rounded. Kumar and Sahni (1986) discussed the fusion of the mandibular alveolar canals in *Andrewsiphius* (their *Remingtonocetus harudiensis*). This fusion is the result of the loss of

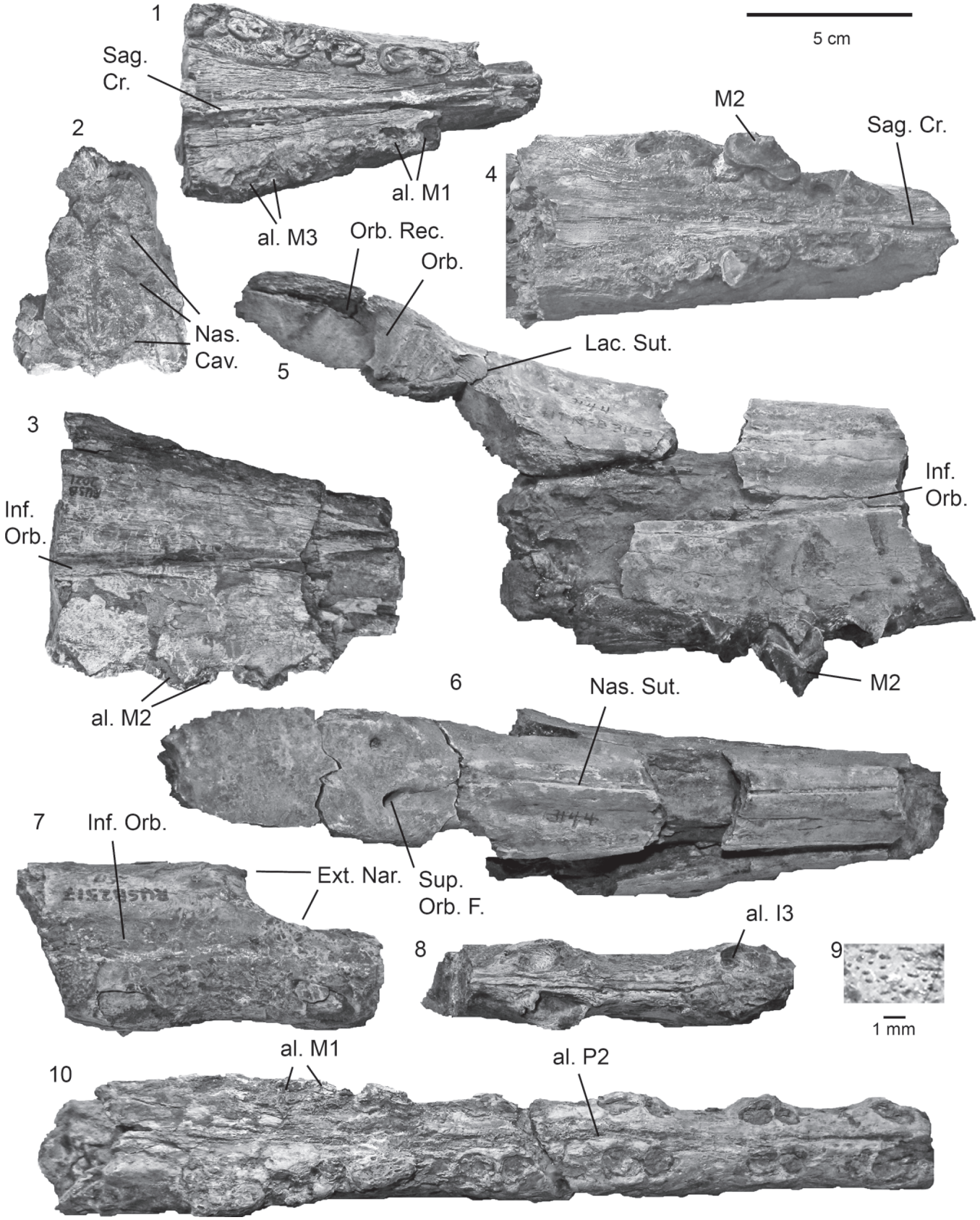

FIGURE *1*—Upper jaws of *Andrewsiphius sloani* (Sahni and Mishra, 1972). *1–3*, occlusal, caudal, and right lateral view of palate and preorbital region (IITR-SB 2021); *4–6*, occlusal, right lateral, and dorsal view of rostrum with palate, preorbital, and orbital region (IITR-SB 3153); *7–8*, right lateral, and occlusal view of premaxilla. Note absence of alveolus for I3 on left side, where a small tooth remains unerupted (IITR-SB 2517); *9*, close-up of surface pitting near premaxillo-nasal suture in IITR-SB 2517, image of area 2 cm behind nasal opening; *10*, occlusal view of gypsified rostrum (IITR-SB 2724). Abbreviations: **al**, alveolus(i) for identified tooth; **Ext Nar**, edge of external nares; **Inf Orb**, infraorbital groove; **Lac Sut**, suture for lacrimal on maxilla; **Nas Cav**, edge of nasal cavity; **Nas Sut**, internasal suture; **Orb**, orbit; **Orb Rec**, orbital recess with two foramina; **Sag Cr**, sagittal crest of palate; **Sup Orb F**, supraorbital foramen. Scale bar near 9 pertains to that figure only.

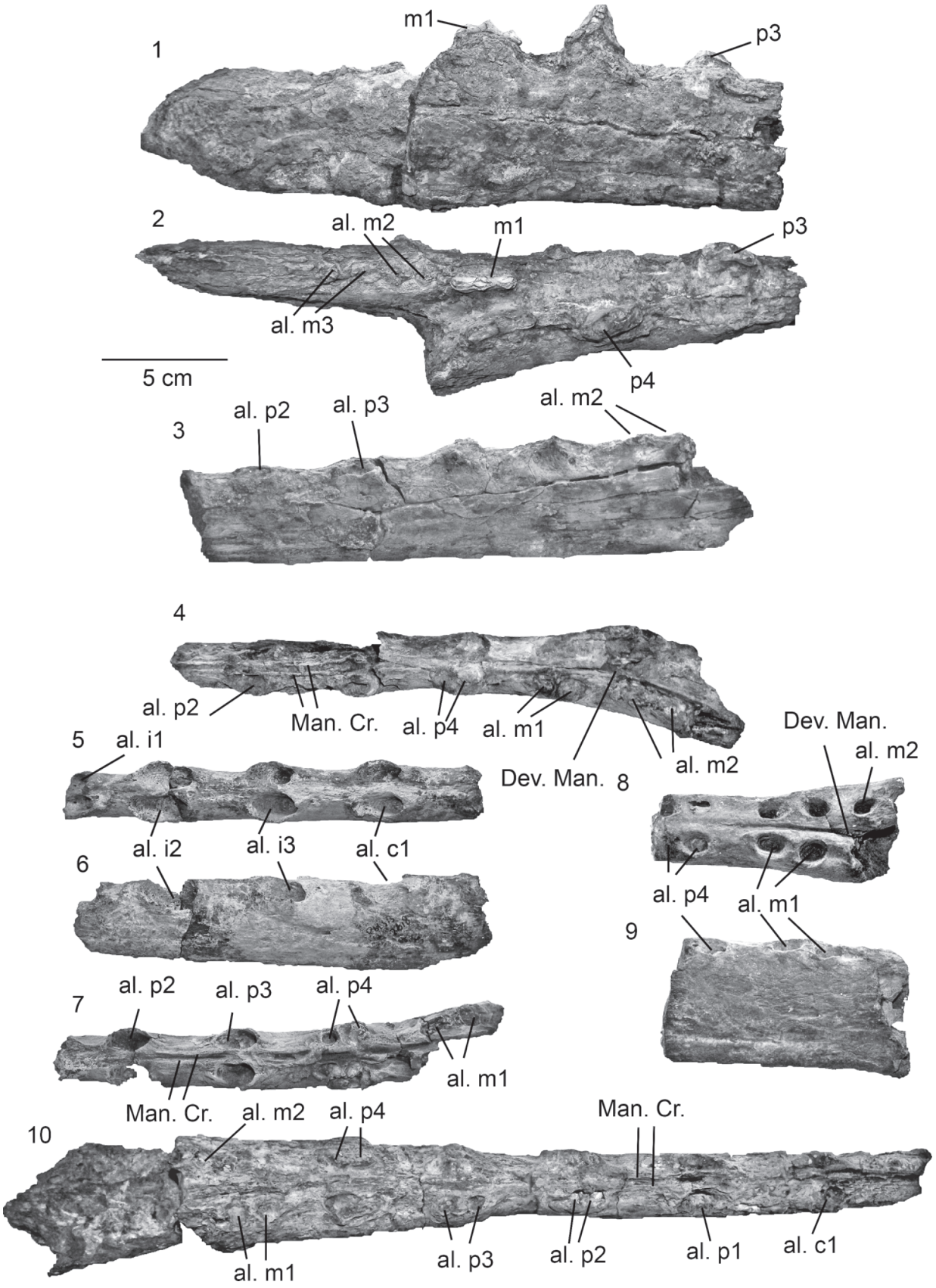

FIGURE 2—Mandibles of *Andrewsiphius sloani* and *Kutchicetus minimus* Bajpai and Thewissen, 2000. *1*, *2*, right lateral and occlusal view of mandible of *Andrewsiphius* (IITR-SB 2723); *3*, *4*, left lateral and occlusal view of mandible of *Kutchicetus* (IITR-SB 2629); *5*, *6*, occlusal and left lateral view of mandible of *Kutchicetus* (IITR-SB 2618); *7*, occlusal view of mandible of *Kutchicetus* (IITR-SB 2780); *8*, *9*, occlusal and left lateral view of mandible of *Andrewsiphius sloani*, holotype (LUVP 11002); *10*, occlusal view of gypsified mandible of *Andrewsiphius*, holotype of *A. kutchensis* (LUVP 11060), junior synonym of *A. sloani*. Abbreviations: **al**, alveolus for identified tooth; **Dev Man**, end of mandibular symphysis on dorsal side; rami deviate from here. **Man Cr**, paired mandibular sagittal crest.

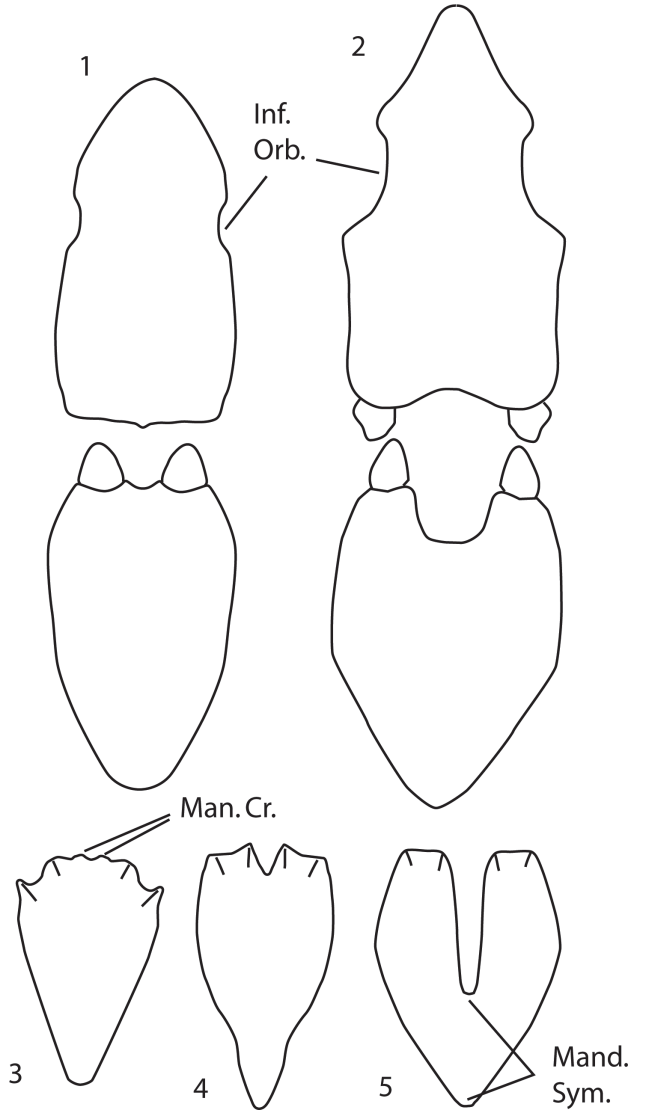

FIGURE 3—Diagrammatic cross-sections through the mandible and maxilla of *Andrewsiphius* and *Kutchicetus* based on tracings of casts. *1*, *2*, sections at the level of p3 and m1 of *Andrewsiphius* (maxilla in 1 based on IITR-SB 2907, in 2 on IITR-SB 3153, mandible in both based on IITR-SB 2723); *3*, *4*, *5*, mandibular sections at the level of p3, m1, and m2 for *Kutchicetus* (IITR-SB 2629). Abbreviations: **Inf Orb**, groove of infraorbital canal; **Man Cr**, bilateral mandibular sagittal crest; **Mand Sym**, ventrally fused mandibular symphysis.

much of the mandibular bone that forms the mandibular symphysis. The canals are clearly fused in LUVP 11002 and 11132. In other specimens, the wall is present but thin (IITR-SB 2650). The size of the mandibular canal suggests that the mandibular foramen is large in *Andrewsiphius*. In IITR-SB 2650, the canal is 21 mm high at 70 mm behind m3. At that point the mandible is 52 mm high. The lateral side of the mandible usually bears a groove for a mental nerve parallel to its inferior edge in *Andrewsiphius* and *Kutchicetus*. The maxilla also bears a groove that extends rostrocaudally for the infraorbital neurovascular group (Fig. 3.1–2, Inf. Orb.). However, the infraorbital groove extends along the dorsoventral middle of the jaw, not near its ventral edge as the mandibular groove does (see Fig. 3.4). This feature can be used to distinguish maxillae from mandibles.

Holotype.—LUVP 11002 (Fig. 2.8–9), left and right mandibular fragment fused at the symphysis, with alveoli for left and right p4 and m1, and right m2. These alveoli were identified as for c1–p3 in the type description (*Remingtonocetus sloani* Sahni and Mishra, 1972). Kumar and Sahni (1986) identified these alveoli as for p2–p4 (interpreting them, correctly, as three double-rooted teeth). The holotype is from Rato Nala (see Thewissen and Bajpai, 1998), a dry streambed between the villages of Baranda (to the northwest) and Harudi (to the south). In the type description, this locality is described as "3 km SE of Baranda," and it is also referred to as "Harudi" (L.U. 2003; Sahni and Mishra, 1975). The Harudi Formation is exposed for several kilometers in the east-west extending Rato Nala.

Referred material.—LUVP 11060 (mandible with alveoli for left and right i3–m2, holotype of *A. kutchensis*; Fig. 2.10; Nareda); LUVP 11132 (mandibular fragment with left and right alveoli for p4–m2; Nareda); LUVP 11165 (maxillary fragment with left and right alveoli/roots for P4–M1 and poor crowns for left M2–M3; holotype of *A. minor*; Rato Nala); IITR-SB 2021 (right and left palatal fragment with alveolus for right P4 and roots for left and right M1–M3; Fig. 1.1–3; Rato Nala); IITR-SB 2031 (maxilla with alveoli for left and right C–P4; Babia Hill); IITR-SB 2517 (rostrum fragment with alveolus for right I3, remnant of left dI3?, and left and right C, and posterior nasal opening; Fig. 1.7–9; Rato Nala); IITR-SB 2526 (mandibular fragment with left and right p4–m1, right alveolus for m2; mandibular fragment with three alveoli; Rato Nala); IITR-SB 2534 (gypsified braincase with left and right bulla, paroccipital process and occipital condyles; tentatively referred, could also be *Kutchicetus*; Babia Hill); IITR-SB 2600 (paroccipital process; Dhedidi South); IITR-SB 2648 (mandibular fragment with alveoli for p4–m1; Godhatad); IITR-SB 2650 (mandibular fragment with left alveoli for p3–m3, right ramus with mandibular foramen; Rato Nala); IITR-SB 2701 (maxilla with roots for left and right P2–P3; Babia Hill); IITR-SB 2712 (mandibular fragment with left and right alveoli for i2–i3; Godhatad Dam): IIT-SB 2723 (mandibular fragment with right alveolus for p3 and well-preserved crowns for right p4 and m1, and left alveoli for p3–m3, with poor crowns for right p3 and m1; Figs. 1.1–2, 5.3; Babia Hill); IITR-SB 2724 (rostrum fragment with alveoli for left and right P1–M3, poor crowns for left and right M1 and left M3; Fig. 1.10; Babia Hill); IITR-SB 2725 (rostrum fragment with alveoli for left C–P2 and right C–P3, also poor crown for right C; Babia Hill); IITR-SB 2742 (associated skull fragments: dorsal nasal and maxillary fragment lacking alveoli, nasal and maxillary fragment with alveoli/roots for left and/or right C, P2, P3, and M1, and crowns for P4 and M2, left and right orbits, occipital condyles, paroccipital process, and many smaller fragments; Akri); IITR 2751 (Two large fragments of a skull, with missing rostrum and dorsal surface, rostrum partly preserved as casts in sediment; rostrum fragment includes alveoli for right P2 and P3, and left P3; braincase and orbital fragment includes well-preserved basicranium, pterygoid region, mandibular fossae and left zygomatic arch, and posterior palate with crowns for right M3, left and right M2, and posterior part of right M1; Fig. 5.2; Rato Nala); IITR-SB 2786 (associated skull fragments: right maxillary fragments with alveoli for P4–M3, occipital condyles, braincase fragment, petroso-squamosal region; Panandhro Lignite Mine); IITR-SB 2787 (left and right mandibular fragment with incisor alveoli; Panandhro Lignite Mine, found on Panandhro Formation outcrops, but probably washed down from overlying Harudi Formation outcrop as suggested by color and preservation); IITR-SB 2793 (gypsified maxilla with crown remnants for left M2–M3, and roots for right M2–

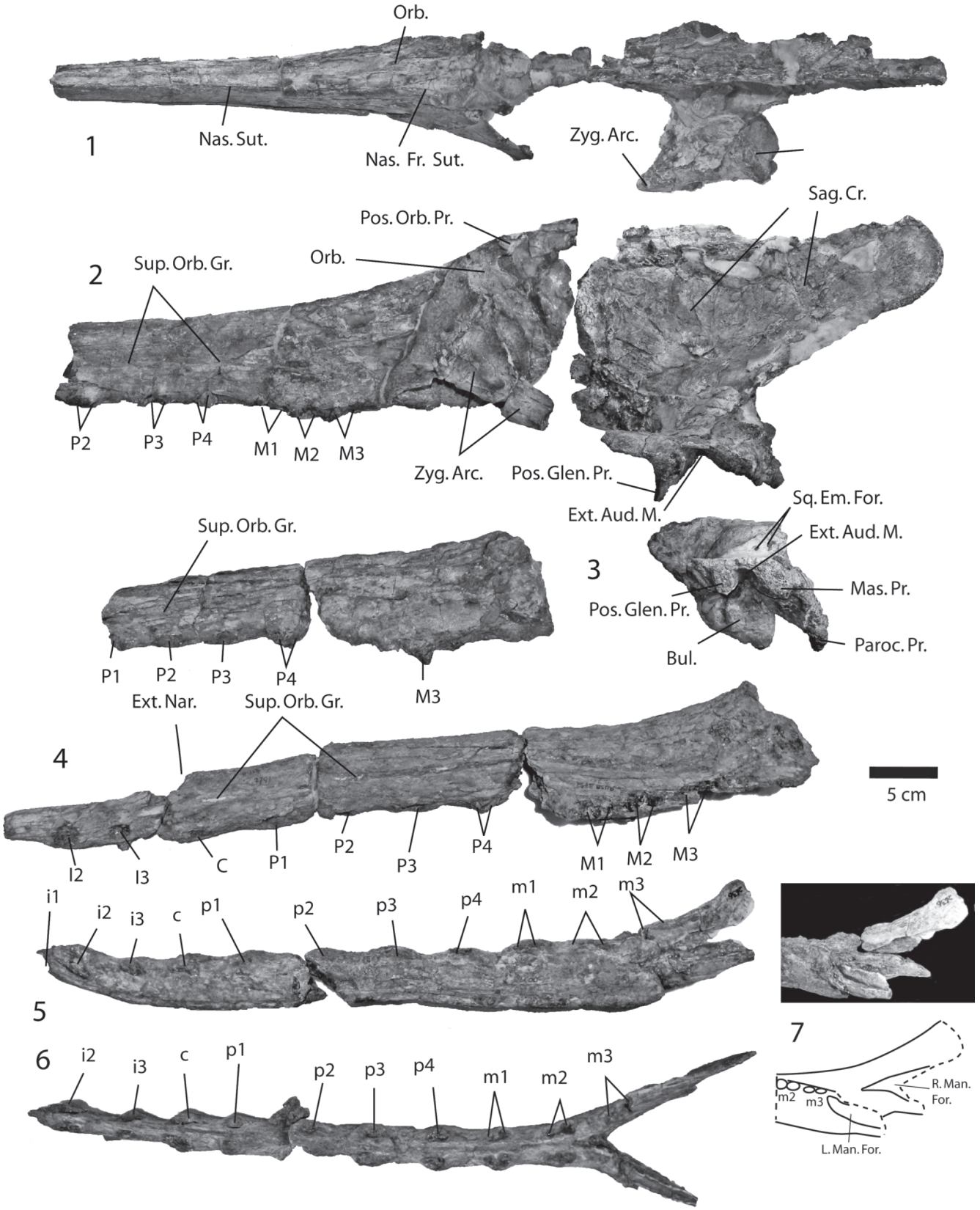

FIGURE 4—Crania and mandibles of *Andrewsiphius sloani* and *Kutchicetus minimus*. *1*, *2*, skull of *Andrewsiphius* in dorsal and lateral view (IITR-SB 2907). Sagittal crest is complete but slightly displaced to the right and ventrally; *3*, gypsified skull of *Kutchicetus* in lateral view, postorbital region not recovered (VPL 1007); *4*, gypsified facial skeleton of *Kutchicetus* in lateral view (IITR-SB 2791); *5–7*, gypsified mandible of *Kutchicetus* in lateral and occlusal view (IITR-SB 2636), and detail of mandibular foramen, with explanatory diagram for 7. Scale bar does not pertain to 7, which is highly foreshortened to show mandibular foramen.

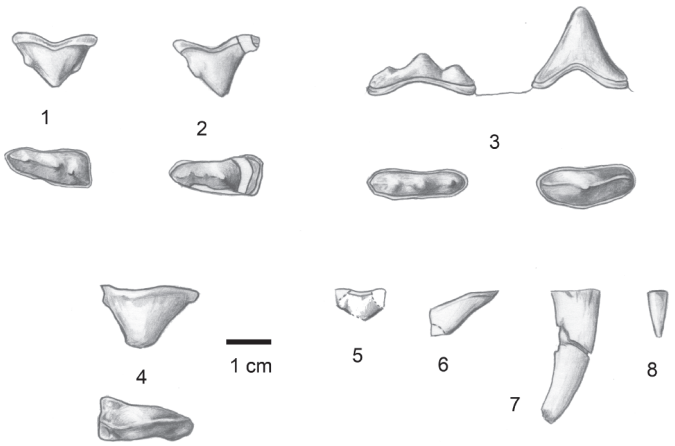

FIGURE 5—Dentition of *Andrewsiphius sloani* and *Kutchicetus minimus*, in buccal and occlusal (1–4) or only in buccal view (5–8), lingual to top of page in all occlusal views. *1*, right M2 of *Andrewsiphius* (IITR-SB 3153); *2*, right M3 of *Andrewsiphius* (IITR-SB 2751); *3*, right p4 and m1 of *Andrewsiphius* (IITR-SB 2723); *4*, left M3 of *Kutchicetus* (VPL 1007); *5–8*, right upper molar fragment (reversed from left), right P4? fragment, right canine, and incisor (respectively IITR-SB 2647.75, .77, .74, and .58) of *Kutchicetus minimus* holotype.

M3; Babia Hill) IITR-SB 2794 (mandibular fragment with two alveoli on left and right side, for two teeth of i2–p1; Babia Hill); IITR-SB 2817 (gypsified braincase, tentatively referred, could also be *Kutchicetus*; Babia Hill); IITR-SB 2827 (mandibular fragment with alveoli for left and right i2; Godhatad); IITR-SB 2833 (mandibular fragment with alveoli for left and right d2, and unerupted crowns for p3; Rato Nala, tentatively referred); IITR-SB 2866 (gypsified maxilla with right roots for p3–m3 and left roots for p1–p2; Lakhpat); IITR-SB 2846 (maxillary fragment with alveoli for I2 and I3; Rato Nala); IITR-SB 2869 (mandibular fragment with left and right alveoli for p3–m2; Dhedidi North); IITR-SB 2871 (associated skeletal elements, see Appendix 1 for list; Godhatad); IITR-SB 2879 (gypsified braincase, tentatively referred, could also be *Kutchicetus*; East of South Pit); IITR-SB 2907 (skull with complete sagittal and nuchal crests, tip of rostrum missing; Fig. 4.1–2; Rato Nala); IITR-SB 2923 (maxilla with roots for P2 to M2; Rato Nala); IITR-SB 2930 (gypsified braincase, tentatively identified, could also be *Kutchicetus*; Babia Hill); IITR-SB 2951 (maxilla with alveoli or roots for P4–M3; Babia Hill); IITR-SB 2979 (cranial fragments including orbits and part of maxilla: Dhedidi North); IITR-SB 3093 (gypsified rostrum fragment with alveoli for left and right P1–P3; Godhatad); IITR-SB 3153 (braincase with left mandibular fossa and both bullae, detached on right side; rostrum fragment with supraorbital region, roots for all molars, and crown for M2; Figs. 1.4–6, 5.2, 6.4–7; Panandhro Lignite Mine); VPL 1019 (rostrum in two fragments, posterior palate with alveoli for left and right P3–M3, and fragment with alveoli and crown/roots for left and right C–P2; Babia Hill). The localities Panandhro Lignite Mine and Akri sample the Panandhro Formation, all others sample the Harudi Formation.

Occurrence.—Middle Eocene (Lutetian) of western India and central Pakistan.

Discussion.—The type specimen of *Andrewsiphius kutchensis* (LUVP 11060, Fig. 2.10) is a mandible with alveoli and tooth fragments for i3 to m2. The type description identified the teeth as i2–m1, but based on more nearly complete material, it is now clear that these alveoli are actually for i3 to m2. Figure 3 of the type description (Sahni and Mishra, 1975) is misleading in that the tooth labeled as p1 (actually p2) is indicated as having a single root, whereas in fact it is double-rooted. Although correctly identified as a mandible in the type description, this gypsified specimen was held to be a maxillary fragment by Gingerich et al. (2001a). It lacks nasal passages, and is thus mandibular. LUVP 11060 was found at Nareda (Locality LU 2005 of Sahni and Mishra, 1975) near Godhatad. This locality is near the village of Nareda (as spelled on the Survey of India toposheets). The name of this village is locally pronounced as "Naredi." However, this is not the village of Naredi of the Survey of India toposheets, the type area of the Naredi Formation (near the village of Baranda). It appears then that the names 'Naredi' and 'Nareda' have been interchanged on the Survey of India maps.

The type specimen of *Andrewsiphius minor* (LUVP 11165) is a badly gypsified rostrum fragment with alveoli/roots for left and right P4 and M1, and poorly preserved crowns for M1–M2. This specimen was held to be a mandibular fragment by Sahni and Mishra (1975), but clearly shows depressions for the frontal sinuses and nasal passages on its posterior side. The specimen was correctly identified as a maxillary fragment by Gingerich et al. (2001a).

Kumar and Sahni (1986) described LUVP 11132 as a paratype mandible with p1–p4 of *Remingtonocetus harudiensis*. The specimen cannot be a paratype because it was not mentioned in the type description of that species. Moreover, it pertains to a cetacean with a narrow, flat palate, unlike *Remingtonocetus* but like *Andrewsiphius*. In size, it matches *A. sloani*.

In the type description of *P. sloani*, two more specimens from the type locality were added to *P. sloani*, but these do not pertain to *Andrewsiphius sloani*. Instead, LUVP 11001 is a skull of *Remingtonocetus*. LUVP 11003 is a large mandible fragment with five alveoli, referred to *Protocetus sloani* by Sahni and Mishra (1972, 1975). We interpret the alveoli of this specimen as those of p4, m1, and anterior m2. The mandible is more robust than that of remingtonocetids, and the proportions of the teeth are different from those of *Remingtonocetus*. It may represent a protocetid. Sahni and Mishra (1975) identified a gypsified braincase (LUVP 11146) as *P. sloani*. This specimen pertains to the genus *Remingtonocetus*. The same authors referred a maxillary fragment (LUVP 11043) to *P. sloani*. We could not locate this specimen, but from the figure in the original publication, the fossil appears to not pertain to *Andrewsiphius*.

Genus *KUTCHICETUS* Bajpai and Thewissen, 2000

Kutchicetus BAJPAI AND THEWISSEN, 2000, p. 1478.

Andrewsiphius BAJPAI AND THEWISSEN, 1998, p. 221 (in part); GINGERICH, UL-HAQ, KHAN, AND ZALMOUT, 2001a, p. 287 (in part).

Type and only species.—*Kutchicetus minimus* Bajpai and Thewissen, 2000.

Diagnosis.—The p2, p3, P2 and P3 single-rooted. Lower molars separated by diastemata. Mandible (left plus right) wider than high near posterior premolars. Mandible and maxilla narrow, flaring buccally to accommodate roots of premolars. Lumbar vertebrae longer and wider than posterior thoracic vertebrae.

Occurrence.—Middle Eocene (Lutetian) of western India.

Discussion.—*Kutchicetus* was first recognized as a new, small cetacean by Bajpai and Thewissen (2000), who described a single specimen with poor cranial and dental but well-preserved and relatively complete postcranial material. Bajpai and Thewissen (2002) tentatively referred several teeth from an older horizon (the Panandhro Formation, previously included

in the Naredi Formation) to this taxon. Gingerich et al. (2001a) synonymized *Kutchicetus* with *Andrewsiphius* based on the argument that the size difference between *A. sloani* and *K. minimus* is minimal. However, in the absence of postcranial material for *Andrewsiphius*, Gingerich et al. (2001a) assumed that *Andrewsiphius* and *Remingtonocetus* had similar proportions, and they used the latter taxon to estimate vertebral dimensions of the former. Their assumption is incorrect: vertebrae and other postcranials of *A. sloani* and *K. minimus* are different in size (as described in the section on postcranial anatomy). In addition, as is clear now, there are important morphological characters distinguishing *Kutchicetus* and *Andrewsiphius*, as outlined in the diagnosis. Dental and cranial dimensions of these taxa are similar, although the mandibles of most specimens of *Kutchicetus* are more slender than those of *Andrewsiphius*.

KUTCHICETUS MINIMUS Bajpai and Thewissen, 2000
Figures 2.3–7, 3.4–5, 4.3–7, 5.4–8, 6.1–3, 8.5, 8.7–13, 9.1–8, 10.1–2, 10.5–10, 10.12–13, and 12

Andrewsiphius kutchensis BAJPAI AND THEWISSEN, 1998, p. 221, figs. 4D, 6A–F, and 7A–B (in part).
Kutchicetus minimus BAJPAI AND THEWISSEN, 2000, p. 1478, figs. 1 and 3.

Diagnosis.—*Kutchicetus minimus* is the only species of its genus and specific and generic features cannot be differentiated.

Description.—This description focuses on rostrum and teeth; other cranial and postcranial material is described below. The dental formula is 3.1.4.3/3.1.4.3. There are diastemata between all lower teeth, including the molars (IITR-SB 2541, 2617). The first lower incisor is smaller than i2 and i3, based on its alveolus (IITR-SB 2618, 2636; Fig. 2.5), and the alveolus for c1 is only slightly larger than those for i3 and p1. Lower p1–p3 are always single-rooted (Fig. 4.5–6) and p4 may have one or two roots. In IITR-SB 2636, the i1–p4 are single-rooted (Fig. 4.6), the lower molars double-rooted. In IITR-SB 2617, p4 is double-rooted on the left side, and the right alveolus for p4 is elongate and partly divided by a septum (suggestive of two roots).

The upper jaw is best preserved in IITR-SB 2791 (Fig. 4.4). This specimen is badly gypsified but shows all alveoli from I1 to M3 in left and right jaw, except for the left I2. This tooth was lost in life, and its alveolus is filled with bone. The I1 was small, as based on its alveolus (5.3 mm in diameter, measurements in this specimen approximate due to gypsification). This alveolus opens rostrally, not onto the palate. Among the incisors, I2 has the largest alveolus (18 mm in diameter), and the left and right alveolus of I2 are separated by only 4 mm. The alveolus for I3 is 15 mm in diameter, whereas that of the canine is 13 mm. The alveoli for P1 to P3 are single-rooted and slightly oval in cross-section; their longest dimension varies from 15 to 17 mm. In this specimen, P4 is single-rooted too, and only part of its crown is preserved; it is 19 mm long at its base. Diastemata occur between all teeth rostral to P4; they are similar in length, approximately 30 mm, except for the much shorter diastema between I3 and C, which is 20 mm. A small fragment of the rostrum of IITR-SB 2791 is missing, and hence the length of the diastema between P4 and M1 cannot be determined, although it was clearly present. There are no diastemata between the upper molars (VPL 1007). The upper molars are similar in length, around 20.2 mm as based on their alveoli in IITR-SB 2791. One specimen has a crown for M3 preserved (VPL 1007; length, 24.3 mm, width, 14.1 mm; Fig. 5.4) and was described by Bajpai and Thewissen (1998). M3 has a single high cusp, the paracone, and is triangular in buccal view. The paracone is set more posterior on the crown than in M2. This tooth also has a protocone lobe on the caudolingual side of the crown but lacks the protocone. It is unclear whether small cuspules, such as on M2 in *Andrewsiphius*, are present because the specimen is somewhat gypsified.

Two fragments of anterior teeth of the holotype (IITR-SB 2647; Fig. 5.7–8) merit closer description. In both, the root and much of the crown is preserved, but the tip is missing. Their roots fit the anterior alveoli of a *Kutchicetus* jaw comfortably (e.g., IITR-SB 2636); the smaller (IITR-SB 2647.58) probably represent the first upper incisor and the second (IITR-SB 2647.74) the upper canine. These teeth show that, in spite of its slender lower jaw, crowns of the anterior teeth of *Kutchicetu*s were high and pointed. The canine is robust with a long crown. At the base of the enamel, it is 11.3 mm long and 9.6 mm wide (Fig. 5.7). The incisor (Fig. 5.8) is very small and pointed; at its base it is 5.3 mm by 4.3 mm.

Among the double-rooted cheek teeth of the holotype, two are robust with closely spaced roots and may represent p4 or P4 (Fig. 5.6). These teeth show a basal cingulum and a crest ascending the main cusp from the cingulum. One specimen can be measured; it is 8 mm wide. Three other tooth fragments that are part of the holotype probably represent upper molars (based on their similarity with upper molars of *Andrewsiphius*). In general, these teeth are similar to those described for *Andrewsiphius*. The largest fragment (Fig. 5.5, IITR-SB 2647.75) shows that the metacone is a small cusp located on the postparacrista.

The left and right mandibles of *Kutchicetus* are fused in a firm synostosis for most of their length (Fig. 4.5–6). Near the occlusal border, the mandibles deviate and the mandibular symphysis ends behind m2, and at the inferior border it reaches beyond m3 (IITR-SB 2636; Fig. 4.5–6). The left and right mandibles join ventrally and produce a prominent median crest (Fig. 3.3–5). On the occlusal side, a sharp crest occurs on the occlusal side of the left and right mandible immediately lateral to the median plane, lingual to the teeth. There are thus two parallel crests (Fig. 3, Man. Cr.) between the left and right lower tooth row near the symphysis (IITR-SB 2636), as in *Andrewsiphius* (LUVP 11002, 11132). On the palate of *Andrewsiphius and Kutchicetus* (IITR-SB 2517, 2791), there is a single, median crest, and this is a useful feature in distinguishing upper and lower edentulous jaw fragments. The most nearly complete mandible of *Kutchicetus* (IITR-SB 2636) also includes a fragment of the caudal part of the jaw (Fig. 4.7). This fragment includes the dorsal edge of the mandible with the root of the ascending ramus and the dorsal part of the mandibular canal. The mandibular canal deeply grooves the mandible and nearly extends to its dorsal edge. This implies that the mandibular canal, and its posterior foramen (the mandibular foramen, Man. For.), of *Kutchicetus* is larger than that of *Ambulocetus* and *Pakicetus*, and is nearly as high as in *Remingtonocetus* and modern cetaceans.

IITR-SB 2629 is an unusual specimen in several regards and is questionably referred to *Kutchicetus minimus*. It has, on the left side, one single alveolus followed by twinned alveoli for four teeth, followed by a partial alveolus for one tooth. Traditionally these would be interpreted as single-rooted p2, double-rooted p3–m2, and a partial alveolus for m3. The specimen differs from *Kutchicetus minimus* in that there is no diastema between m2 and m3, although there are diastemata

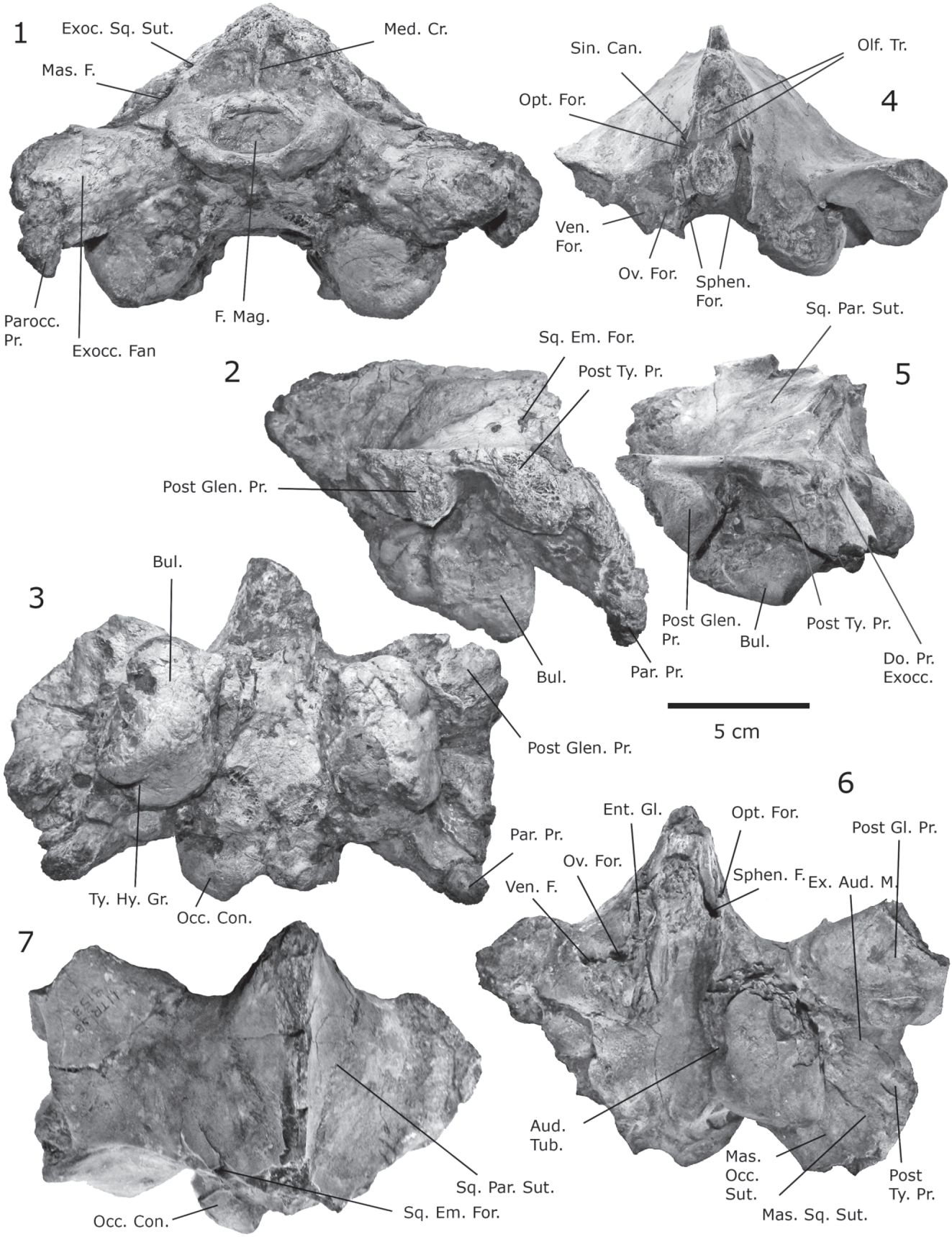

FIGURE 6—Braincases of *Andrewsiphius sloani* and *Kutchicetus minimus*. *1–3*, occipital, left lateral, and ventral view of braincase of *Kutchicetus minimus* (VPL 1007); *4–7*, rostral, right lateral, rostroventral, and dorsal view of braincase of *Andrewsiphius sloani* (IITR-SB 3153). Abbreviations: **Bul**, bulla; **Do Pr Exocc**, dorsal process of the exoccipital; **Ent Glen**, entoglenoid process; **Ex Aud M**, external auditory meatus; **Exocc Fan**, exoccipital fan;

between all other teeth (and it is therefore also different from *Andrewsiphius sloani*). In addition, the alveolar length of p3 is much greater on the right side (19 mm), than on the left side (11 mm). This specimen may represent a new species or an aberrant specimen (e.g., with retained deciduous molars).

Holotype.—IITR-SB 2647, partial skeleton (Figs. 5.5–8, 8.5, 8.11–13, 9.4–8, 10.1–2, 10.5–10, 10.12–13, and 12), including dental, cranial, and postcranial fragments (see Appendix 1 for list of elements). The most significant cranial parts are a maxillary fragment with sutures for the nasals and alveoli for left and right P1 and C1 and a depression, filled with bone fragments of the lower jaw in the sediment. The holotype was recovered in the Harudi Formation near Godhatad, just south of the road between the villages Godhatad and Nareda, as described in Bajpai and Thewissen (2000). The type site is approximately 50 m south of this road, and 100 m east of a broad and shallow dry (in winter) riverbed covered with thorny shrubs. It occupies an area of approximately 5 by 10 meters, and more bones have weathered/excavated out off the marly limestone since the holotype was published. Hence, the description below includes more elements than the type description (Bajpai and Thewissen, 2000). Annual collecting following the monsoon season continues and it is likely that more elements will be recovered in the future.

Referred material.—IITR-SB 2541 (mandibular fragment with alveoli for left and right m1, Babia Hill); IITR-SB 2590 (left P1; Panandhro Lignite Mine, tentatively referred); IITR-SB 2617 (mandibular fragment with alveoli for right p4 and m1, and left p4–m2, Godhatad); IITR-SB 2618 (mandibular fragment with left and right alveoli for i1–c; Fig. 2.5–6; Godhatad); IITR-SB 2629 (mandibular fragment with alveoli for left p2–m3 and right p2–p4, questionably referred; Fig. 2.3–4; Babia Hill); IITR-SB 2636 (complete edentulous left and right mandibular ramus with alveoli for left and right i1–m3; Fig. 4.5–7; Babia Hill); IITR-SB 2780 (left and right mandible with alveoli for left and right p2–m1 and left p2–p4; Fig. 2.7; Panandhro Lignite Mine); IITR-SB 2791 (rostrum with roots for left and right I1, left I2 [right I2 alveolus is covered by remodeled bone], partial crown for I3, alveoli for right and left I3–M3, partial orbit; Fig. 4.4; Babia Hill); IITR-SB 2949 (mandibular fragment with base of left and right m1 and alveoli for left and right m2–m3; Babia Hill); IITR 3100 (rostrum fragment with alveoli for M1 and M2; Lakhpat); VPL 1007 (three associated skull fragments: braincase; posterior rostrum and orbit fragment with alveoli for right M1–M3, left M1–M2, and crown for left M3; rostrum fragment with alveoli for left P1–P4 and right P2–P3 with poor crown for right P4; Figs. 4.3, 5.4, 6.1–3; Babia Hill). The Panandhro Lignite Mine Locality yields fossils from the Panandhro Formation, all other fossils are from the Harudi Formation.

Occurrence.—Middle Eocene (Lutetian) of western India.

Discussion.—*Kutchicetus* is clearly distinct from *Andrewsiphius* in re a single-rooted P1–P3 and p1–P3, and a jaw that is slender. Based on single specimens of the postcranial skeleton described below, *Kutchicetus* is also smaller postcranially than *Andrewsiphius*, but differences in cranial size are small. *Kutchicetus* is an unusual mammal, retaining a complete dental formula but reducing most of the cheek teeth in size; many of its teeth are single-rooted and even the lower molars are separated by diastemata. The tooth crowns found with the holotype indicate that the anterior teeth (incisor, canines) were long and pointed, whereas the molars had low crowns.

Bajpai and Thewissen (2002) recovered six cetacean teeth from the Panandhro Formation of the Panandhro Lignite Mine, and referred one of these to '*Kutchicetus minimus?*' This specimen, IITR-SB 2590, is a single-rooted premolar, the root of which fits alveoli of *Kutchicetus* specimens.

CRANIAL OSTEOLOGY

The skull of *Andrewsiphius* (Figs. 4.2 and 11) has a long and very narrow rostrum, eyes that are set high on the skull and close together, a downsloping zygomatic arch and low mandibular fossa, and an enormous sagittal crest that is higher than the braincase and overhangs the nuchal plane significantly. Condylobasal length in *Andrewsiphius* was determined, prior to excavation, to be 56 cm in IITR-SB 2751 (Fig. 7.1), where several parts of the jaw were preserved as casts in the surrounding sediment. Known skull fragments for *Kutchicetus* (Fig. 4.3–4) do not give a complete picture of its skull, but they suggest that it was similar to *Andrewsiphius*. The nasal opening in *Andrewsiphius* and *Kutchicetus* extends posteriorly over the diastema between I3 and C (IITR-SB 2517, 2791, Figs. 1.7–8 and 4.4: Ext. Nar.). Rostral to this, the premaxilla is narrow and pointed (IITR-SB 2791). Premaxilla and maxilla are extremely narrow (Fig. 3.1–2), and the maxilla at M3 is approximately twice as high as the entire width of the palate (Fig. 1.1–3). The surface texture of the tip of the rostrum is unusual in that it shows a great number of small foramina (Fig. 1.9). These foramina may have housed nerves to whiskers or sensory organs similar to those of crocodiles and shorebirds (Dehnhardt and Mauck, 2008). Similar foramina were observed previously by Thewissen and Nummela (2007) in pakicetids.

The palate is also narrow and flares laterally to accommodate incisors, canine, and premolars (Fig. 1.8 and 10, Fig. 11). In many cases, alveoli for the same tooth on left and right side are off-set (Fig. 1.8), leaving the maxilla narrower yet (VPL 1007, IITR-SB 2517). The palate bears a prominent sagittal crest (Fig. 1.1, Sag. Cr.; Fig. 3.1), and left and right maxillae meet sharply on the dorsal side of the rostrum. The infraorbital foramen (Fig. 1.5: Inf. Orb.) is near the junction between M2–M3 (VPL 1007, IITR-SB 2907), and a groove extends anteriorly from this foramen onto the rostrum up to the area over the canine (Figs. 1.5 and 11). This groove housed the infraorbital neurovascular group. The premaxilla-maxilla suture crosses the alveolus near the canine and extends dorsocaudally (IITR-SB 2517) but cannot be followed further dorsally (Fig. 11). The nasal suture (Fig. 1.6: Nas. Sut.) is visible rostrally near the nasal opening. It extends dorsocaudally, and the nasals form a narrow roof of the rostrum (Fig. 1.6; IITR-SB 2517, Fig. 3). The nasal suture is visible dorsal to the molars (IITR-SB 2021, 2907). Here the nasals widen and make up a larger part of the side of the face, and they contact the lacrimal. The most caudal extent of the nasals is immediately rostral to the large supraorbital foramina

←

Exocc Sq Sut, suture between exoccipital and squamosal; **Mas F**, mastoid foramen; **Med Cr**, median crest on supraoccipital; **Occ Con**, occipital condyle; **Olf Tr**, Cast of olfactory tract; **Opt For**, optic foramen; **Ov For**, oval foramen; **Par Pr**, paroccipital process; **Post Glen Pr**, postglenoid process; **Post Ty Pr**, posttympanic process; **Sin Can**, sinus canal; **Sphen F**, sphenorbital foramen; **Sq Em For**, squamosal emissary foramen; **Sq Par Sut**, squamosal parietal suture; **Ty Hy Gr**, groove for tympanohyal; **Ven For**, venous foramen.

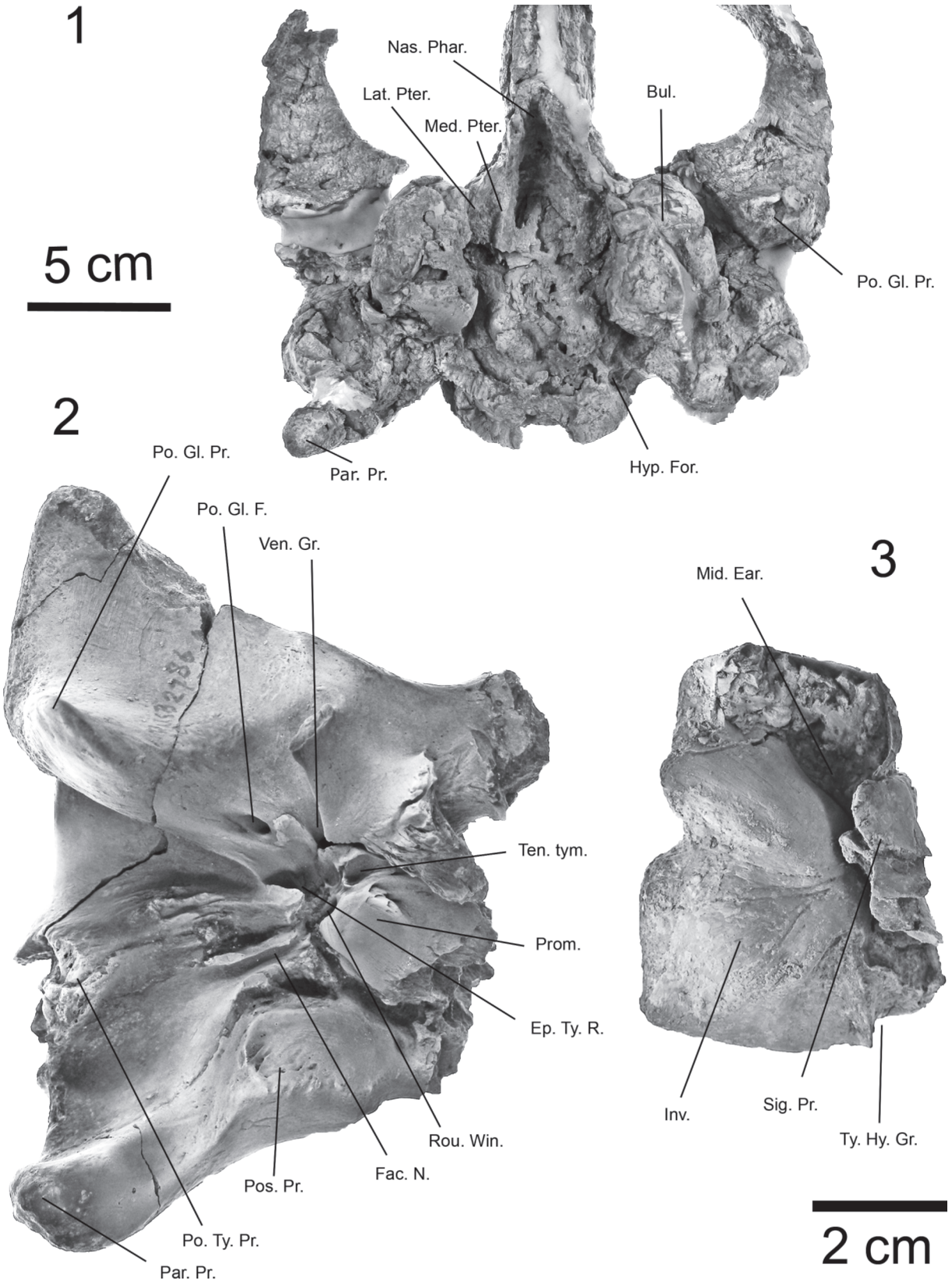

FIGURE 7—Basicranium, ear region, and tympanic of *Andrewsiphius*. *1*, ventral view of basicranium (IITR-SB 2751); *2*, ventral view of right ear region with tympanic removed (IITR-SB 2786). *3*, dorsal view of right tympanic removed from skull (IITR 3153). Abbreviations: **Bul**, Tympanic bulla; **Ep Ty R**, epitympanic recess; **Fac N**, facial nerve; **Hyp For**, hypoglossal foramen; **Inv**, involucrum; **Lat Pter**, lateral pterygoid plate; **Med Pter**, medial pterygoid plate; **Mid Ear**, middle ear; **Nas Phar**, nasopharyngeal duct; **Par Occ Pr**, paroccipital process; **Po Gl F**, postglenoid foramen; **Po Gl Pr**, postglenoid process; **Pos Pr**, process for attachment of posterior process of tympanic; **Po Ty Pr**, posttympanic process; **Prom**, promontorium; **Rou Win**, round window; **Sig Pr**, sigmoid process; **Ten Tym**, groove for Tensor tympani; **Ty Hy Gr**, tympanohyal groove; **Ven Gr**, venous groove on suture between petrosal and squamosal.

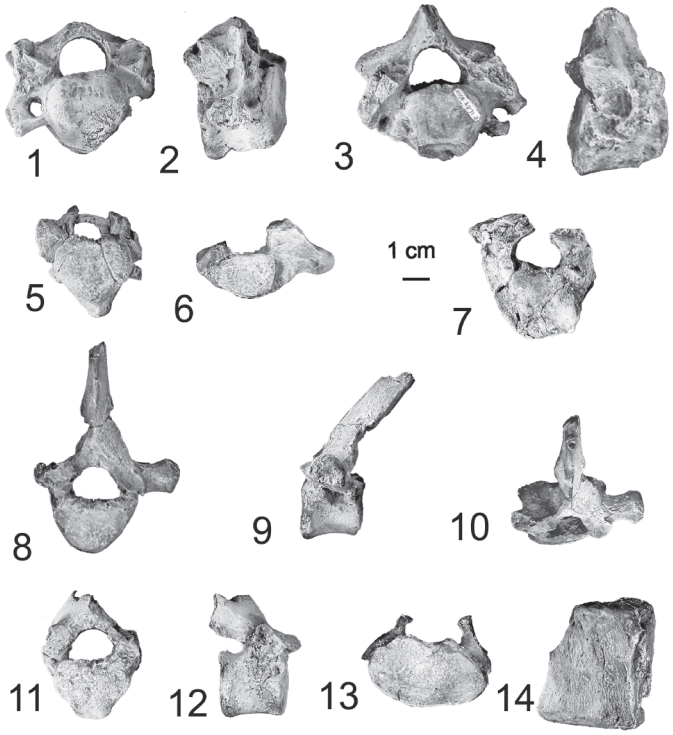

FIGURE 8—Cervical and thoracic vertebrae of *Andrewsiphius sloani* and *Kutchicetus minimus*. *1–4*, cranial and right lateral views of cervical vertebra 6 and 7 of *Andrewsiphius* (IITR-SB 2871.1 and .2, respectively); *5*, cranial view of cervical vertebra 5 of *Kutchicetus* (IITR-SB 2647.71); *6*, cranial view of thoracic vertebra 10 of *Andrewsiphius* (IITR-SB 2871.38); *7*, cranial view of thoracic vertebra 2 of *Kutchicetus* (IITR-SB 2871.2); *8–10*, cranial, left lateral, and dorsal view of thoracic vertebra 11 of *Kutchicetus* (IITR-SB 2871.7); *11–12*, cranial and right lateral view of thoracic vertebra 13 of *Kutchicetus* (IITR-SB 2647.8); *13*, cranial view of lumbar vertebra 8 of *Kutchicetus* (IITR-SB 2647.12); *14*, ventral view of lumbar vertebra 8 of *Andrewsiphius* (IITR-SB 2871.8).

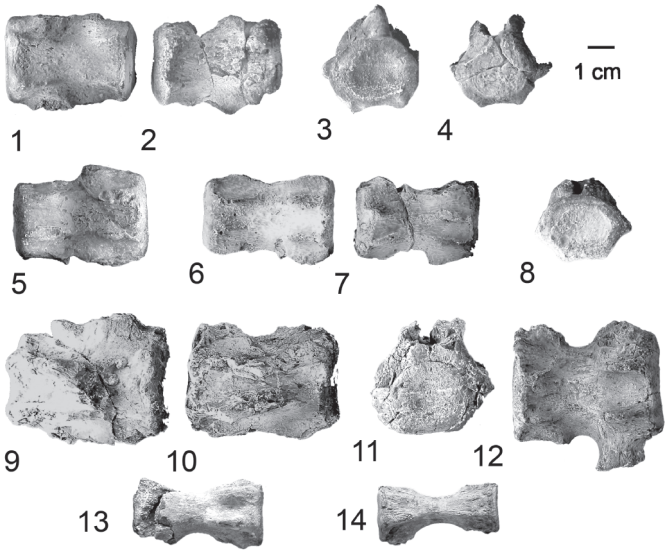

FIGURE 9—Central and terminal caudal vertebrae of *Kutchicetus minimus* and *Andrewsiphius sloani*. *1–3*, ventral view of caudal vertebrae 9 and 10 (IITR-SB 19 and 201), and posterior view of caudal vertebra 9 of *Kutchicetus*; *4–5*, anterior and ventral view of caudal vertebra 12 of *Kutchicetus* (IITR-SB 2647.22); *6–8*, ventral view of caudal vertebrae 14 and 15 (IITR-SB 2647.23 and 24), and posterior view of caudal vertebra 14 of *Kutchicetus*; *9–11*, dorsal view of caudal vertebrae 8 and 9 (IITR-SB 2871.7 and 3), and anterior view of caudal vertebra 9 of *Andrewsiphius*; *12*, ventral view of caudal vertebra 10 of *Andrewsiphius* (IITR-SB 2871.16); *13*, ventral view of caudal vertebra 18 of *Andrewsiphius* (IITR-SB 2871.12); *14*, ventral view of caudal vertebra 19 of *Andrewsiphius* (IITR-SB 2871.11).

(Fig. 1.6: Sup. Orb. F.). Medial to this, the frontals project in the median plane between left and right nasals. The lacrimal extends far on the side of the face, the lacrimomaxillary suture is visible as far anterior as M3 (Fig. 1.5: Lac. Sut.) and is lost in a damaged area rostral to this (Fig. 11). The lacrimal foramen is located on the face (IITR-SB 2979).

Inside the orbit, the ventral suture of the lacrimal can be followed for a short distance extending ventrocaudally. No other sutures can be recognized in the orbit. Two foramina occur in the dorsal part of the orbit, where they are located in a common recess (IITR-SB 2742, 2907; Fig. 1.5, Orb. Rec.). The anterior of these is probably the orbital foramen of the supraorbital canal and the posterior is probably the frontal diploic foramen. A crest extends ventrocaudally in the anterior part of the orbital fossa. The area cranial to this is rugose, while the area posterior to this is smooth and concave. The latter area broadens dorsocranially and housed the periorbita. The orbit is a narrow cone, directed steeply dorsal, although the eye faced more laterally than dorsally (IITR-SB 2907; Fig. 11). Anterior to the orbit is the sphenopalatine foramen, located immediately deep to the most dorsal point of the zygomatic arch. Inferior to the orbit is the narrow nasopharyngeal duct, which is ossified until just anterior to the auditory bullae (IITR-SB 2751; Fig. 7.1: Nas. Phar.). It cannot be determined which bones contribute to the nasopharyngeal duct; it is possible that palatine, alisphenoid, and pterygoid are involved. The interorbital region is extremely narrow (Figs. 4.1 and 6.4), and the olfactory tract is long. These conditions occur in all early whales (Thewissen et al., 2007), but the andrewsiphiines appear to be more extreme than other archaeocetes in this respect. The width across the postorbital processes in *Andrewsiphius* (IITR-SB 2907) is 50 mm, whereas the height of the skull at this point is 127 mm. The postorbital processes are wider than the nasopharyngeal duct.

The width of the palate in the incisor region is similar to that in the premolar region. Between the molars (Fig. 1.1 and 4), the palate widens somewhat at M1 but retains its sagittal crest. Two specimens are not gypsified and retain well-preserved palates (IITR-SB 2021 and 3153); in these specimens no greater palatine foramen is apparent. The suture between palatines and maxilla extends on the palate as far rostral as M2 or further (IITR-SB 3153). The palate extends considerably caudal to the molars and is widely and deeply indented by the caudal palatine notch. Dorsal to this notch is the caudal opening of the infraorbital canal. The skull at M2 is very narrow, relative rostrum width (skull width at M2/width across the occipital condyles) in *Andrewsiphius* is 107% (IITR-SB 2907) and 113% (IITR-SB 3153) and in *Kutchicetus*: 82% (VPL 1007).

The zygomatic arch is preserved in IITR-SB 2751 and 2907 (Figs. 4.1–2, 7.1). It is mediolaterally flattened and deep dorsoventrally. It projects strongly ventrocaudally to reach the mandibular fossa, which is placed low on the side of the skull (Fig. 4.1). On the medial side of the zygomatic arch, the suture between maxilla and jugal is visible; it is located 20 mm caudal to the junction of zygomatic arch and nasal wall.

The rostral suture of the squamosal is clear on the right side of IITR-SB 2907 and forms the rostral edge of the braincase (Fig. 11). On the dorsal side of the cranial cavity, at the root of the sagittal crest, the squamosal suture extends caudally (VPL 1007) and reaches the nuchal crest just dorsal to the very large

FIGURE *10*—Limb skeleton of *Kutchicetus minimus* and *Andrewsiphius sloani*. *1*, *2*, caudal and cranial view of left humerus of *Kutchicetus* (IITR-SB 2647.401 and 42); *3*, *4*, caudal view of the right humerus of *Andrewsiphius* (IITR-SB 2871.17 and 201); *5*, *6*, caudal and cranial view of left proximal radius of *Kutchicetus* (IITR-SB 2647.52); *7*, medial view of the left olecranon of *Kutchicetus* (IITR-SB 2647.51); *8*, *9*, caudal and cranial view of left femur of *Kutchicetus* (IITR-SB 2647.41); *10*, cranial view of right femur of *Kutchicetus* (IITR-SB 2647.501); *11*, cranial view of left femur of *Andrewsiphius* (IITR-SB 2871.15); *12*, cranial view of right tibia of *Kutchicetus* (IITR-SB 2647.43 and 44); *13*, ischium and ilium fragments of *Kutchicetus* (IITR-BS 2647.32 and .46), lateral to top of page, acetabulum is located in the missing section; *14*, caudal view of left patella of *Andrewsiphius* (IITR-SB 2871.21).

squamosal emissary foramen (Fig. 6.2: Sq. Em. F.). The suture between frontal and parietal on the side of the skull can be followed in IITR-SB 3153, extending straight dorsally across the root of the olfactory tract. This suture cannot be followed with certainty on the sagittal crest, but a zone of small cracks appears to indicate that it extends more-or-less straight dorsoventrally. Dorsally, this suture is clear in IITR-SB 2742, descending from the sagittal crest approximately 20 mm behind the postorbital process. The root of the zygomatic process projects laterally (IITR-SB 2907, 3153; Fig. 4.1–2), and its caudal edge forms a roof over the external auditory meatus. The zygomatic process is continuous with the mastoid process. A robust tubercle occurs laterally on the base of the postglenoid process (Fig. 7.2: Po. Gl. Pr.). Bilateral width of the skull across the zygomatic process is 209 mm in IITR-SB 2907.

The skull of the andrewsiphiines appears low and broad in caudal view in most braincases because the sagittal crest is lost in many fossils (IITR-SB 2534; 2817; 2879 2930; 3153; VPL 1007). The full height of the sagittal crest is preserved in only one specimen (IITR-SB 2907; Fig. 4.1–2; Sag. Cr.). The sagittal crest greatly overhangs the posterior wall of the braincase. This crest is 90 mm high above the braincase and makes up 57% of the height of the caudal aspect of the skull (Fig. 11). In addition, the nuchal shield is enormous, extending 125 mm beyond the occipital condyles caudally.

The exoccipitals are particularly well-preserved in IITR-SB 3153. In posterior view, the suture between exoccipital and squamosal extends along the inferior side of the nuchal crest, which is low in this area (Fig. 6.1; Exoc. Sq. Sut.). The suture is recessed, and dorsal to the crest is a large, slit-like mastoid foramen (Fig. 6.1: Mas. F.), which deeply grooves the nuchal crest occipitally. This foramen is located across the nuchal crest opposite the large squamosal emissary foramen (Fig. 6.2). The exoccipital flares labially and ventrally as a flat plate (VPL 1007; Fig. 6.1: Exocc. Fan), described as a fan-shaped fossa by Geisler (2001), and ends inferiorly in the paroccipital process (Parocc. Pr.) and laterally in a rugose process here called the dorsal process of the exoccipital (Fig. 6.5: Do. Pr. Exocc.). The inferior tip of the paroccipital process is curved anteriorly into a hook-like shape in andrewsiphiines (VPL 1007, Fig. 6.2). The root of the paroccipital process also forms the root of the dorsal process of the exoccipital (IITR-SB 2795, 2879, 3153, VPL 1007). The occipital condyles are convex and not fused in the ventral midline (IITR-SB 3153). The part of the supraoccipitals that is above the foramen magnum (Fig. 6.1: F. Mag.) is rugose and bears a strong, median crest (Fig. 6.1: Med. Cr.), but it does not possess the tubercles that are present in some other Eocene cetaceans (pakicetids, Nummela et al., 2006). This median crest ends at the level of the roof of the braincase and does not continue onto the nuchal shield. The nuchal shield, formed at the junction of left and right nuchal crest and sagittal crest, faces caudo-ventrally (Fig. 4.1). It is concave in cross-section, tapering into a narrow groove caudally. The left and right nuchal crests meet and join the posterior part of the sagittal crest in a rounded process. Width of the foramen magnum is 28.8 mm in VPL 1007 and 21.7 mm in IITR-SB 3153. Width across occipital condyles is 57 mm in VPL 1007 and 60.7 mm in IITR-SB 3153.

In ventral view, the skull narrows considerably behind the palate. This is the area of the ossified nasopharyngeal duct (Fig. 7.1: Nas. Phar.), a structure usually lost to breakage and absent in most of the preserved skulls. It is preserved in IITR-SB 2751, and projects more ventrally than either the auditory bulla or the paroccipital process. Rostromedially to the ear, the wall of the nasopharyngeal duct divides into lateral and medial pterygoid crests (Fig. 7.1: Lat. Pter. and Med. Pter.), which cradle the large, triangular pterygoid fossa. The basicranium widens here to accommodate ears and zygomatic root. In the area where the skull broadens, three foramina open into the braincase from rostral. These foramina are arranged in a row from dorsal to ventral; the two higher ones are very small and probably represent sinus canal and optic canal (Fig. 6.4 and 6: Sin. Can. and Opt. For.). The lowest foramen is enormous, and represents the sphenorbital fissure (Fig. 6.4 and 6: Sphen. For.). Grooves pass dorsally and rostrally from all three foramina, and the grooves associated with the optic canal and sphenorbital fissure are directed toward the orbit. The root of the lateral pterygoid plate is just lateral to these foramina, and lateral to it are two sediment-filled depressions of similar size in IITR-SB 3153. In IITR-SB 2907, a foramen in this area is on the suture between squamosal and alisphenoid and probably represents the oval foramen (Fig. 6.4: Ov. For.). The canal leading into the cranial cavity from this foramen is exposed in IITR-SB 2786. The medial depression in IITR-SB 3153 may represent a venous foramen (Fig. 6.6: Ven. F.), because a faint trace of a

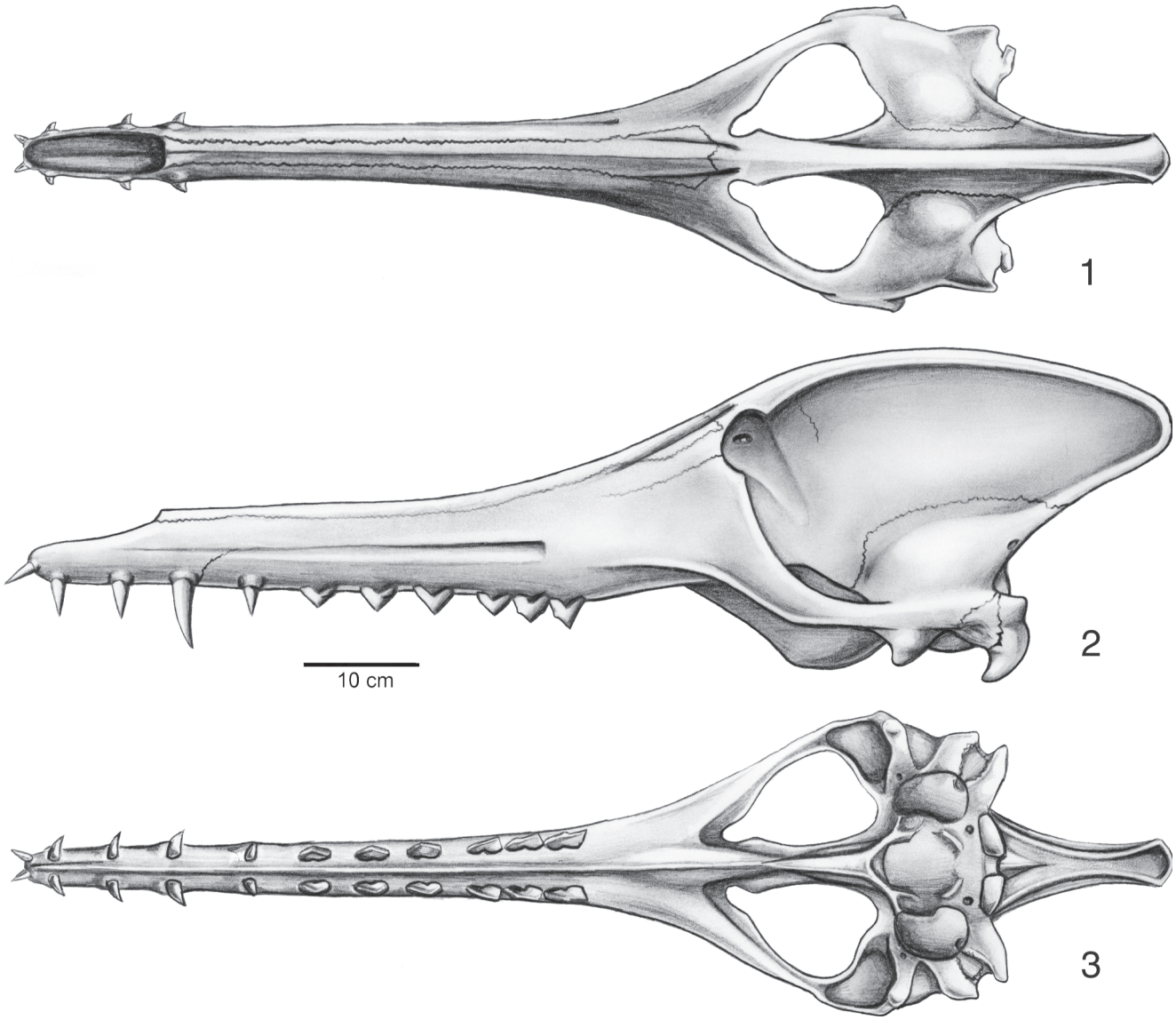

FIGURE *11*—Reconstruction of skull of *Andrewsiphius sloani*, in dorsal (*1*), left lateral (*2*), and ventral (*3*) view by Jacqueline Dillard.

groove extends laterally to the dorsal surface of the zygomatic process. These two foramina are located on a prominent process on the basicranium, and a crest projects from this elevation above each foramen. The auditory bulla articulates with this elevation (IITR-SB 3153), and there is a distinct entoglenoid facet on the lateral surface of the medial crest (Fig. 6.6: Ent. Gl.). The medial side of this elevation is grooved for the auditory tube. Lateral to this elevation is the mandibular fossa, which is triangular in shape and somewhat concave in all directions (IITR-SB 2786; Fig. 7.1). The postglenoid process (Fig. 6.2: Post Glen. Pr.) is narrow and sharp and placed laterally on the mandibular fossa. This leaves a broad connection between the mandibular fossa immediately anterior to the tympanic bulla. Andrewsiphiines had a large fossa in the medial aspect of the mandible (Fig. 4.7), and it is likely that it contained a mandibular fat pad. This pad would have passed medially to the postglenoid process to the medial wall of the tympanic.

The tympanic bulla (IITR-SB 2879; 3153; VPL 1007; Figs. 6.1–3, 7.1 and 3: Bul.) is roughly oval in outline, and has a distinct crest rostromedially, which shields the ventral side of the auditory tube (Fig. 6.6). The bulla is grooved caudally for the tympanohyal (Figs. 6.3 and 7.3: Ty. Hy. Gr.), and has a distinct sigmoid process (VPL 1007; 3153; Fig. 7.3: Sig. Pr.). The involucrum is enormous (Fig. 7.3: Inv.), and the middle ear cavity very small and tapers caudally (IITR-SB 3153: Fig. 7.3: Mid. Ear).

Medial to the bulla is the basioccipital (IITR-SB 3153), which bears prominent tubercles for the rectus capitis muscle but lacks a lateral (falcate) process. The anteromedial edge of the rectus capitis tubercles articulates with the bulla. The hypoglossal foramen is located lateral to these tubercles (Fig. 7.1: Hyp. For.), well anterior to the occipital condyle. Several condylar foramina occur immediately rostral to the occipital condyles and are covered by them from view.

The petrosal is well preserved in IITR-SB 2786 (Fig. 7.2). The promontorium is diamond-shaped (Fig. 7.2: Prom.). One tip of the diamond faces rostrally, and immediately anterior to it is the oval fossa for the tensor tympani muscle (Fig. 7.2: Ten. Tym.). A groove for the motor nerve to tensor tympani extends from this fossa medially on the rostromedial side of the promontorium and connects to the groove that ends in the

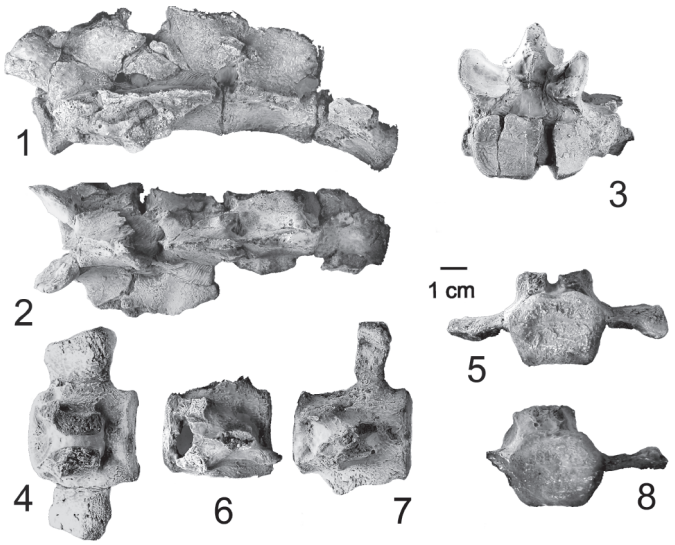

FIGURE *12*—Sacrum and anterior caudal vertebrae of *Kutchicetus minimus*. *1–3*, left lateral, dorsal, and anterior view of sacrum (IITR-SB 2647.13); *4–5*, dorsal and caudal view of caudal vertebra 3 (IITR-SB 2647.16); *6*, dorsal view of caudal vertebra 5 (IITR-SB 2647.17); *7–8*, dorsal and caudal view of caudal vertebra 6 (IITR-SB 2647.18).

oval foramen. A very small foramen is located lateral to the fossa for tensor tympani. It probably represents a small venous foramen connecting to a broad groove that is directed medially to the mandibular fossa (Fig. 7.2: Ven. Gr.), on the suture between petrosal and squamosal. The postglenoid foramen (Fig. 7.2: Po. Gl. F.) is located lateral to this groove, rostromedial to the external auditory meatus.

Rostrolateral to the promontorium is a wide depression, which is larger and reaches more dorsally than that for tensor tympani. This depression is the epitympanic recess (Fig. 7.2: Ep. Ty. R.). This recess is overhung caudally by a sharp process from the squamosal. In its medial wall is a very small foramen for the facial nerve, and a groove for this nerve (Fig. 7.2: Fac. N.) extends caudally along the promontorium, bending abruptly lateral to the lateral tip of the promontorium, to groove the mastoid on its course laterally. The latter groove is overhung anteriorly by a crest of bone from the mastoid. Medial to the foramen for the facial nerve, in the lateral wall of the promontorium, is the oval window.

Caudolateral to the promontorium is a narrow irregular depression. Immediately posterior to this depression is a rounded area on the exoccipital that is elevated (extends ventrally) and has a rugose texture for the attachment of the posterior process of the tympanic (Fig. 7.2: Pos. Pr.). Lateral to this is the hook-like paroccipital process (Fig. 7.2: Par. Pr.). The round window is located in the caudolateral wall of the promontorium (Fig. 7.2; Rou. Win.).

The ventral side of the paroccipital process is a flat plane (VPL 1007). This plane extends rostrally to the tympanic. Rostrally, the paroccipital plane is continued onto the mastoid process as a gently concave depression (Fig. 6.6). The suture between mastoid and exoccipital crosses the middle or the posterior part of the concave area (IITR-SB 2786, 3153, VPL 1007). Rostrally, the depression in the mastoid is bordered by a rugose area: the posttympanic process of the squamosal (Figs. 6.2, 6.6, 7.2: Po. Ty. Pr.). This process varies widely in size and shape, and is low and rugose in IITR-SB 3153 and extends far caudally. On the other hand, it is very high on the right side of VPL 1007 (Fig. 6.2) but does not extend far caudally. It is possible that this is a difference between *Andrewsiphius* and *Kutchicetus*, but a larger sample is necessary to evaluate this. The facial nerve runs on the posterior aspect of this process and is thus directed relatively lateral (IITR-SB 2786, 2879, VPL 1007, Fig. 7.2: Fac. N.). Rostral to the posttympanic process is the external auditory meatus.

POSTCRANIAL OSTEOLOGY

Relatively complete postcranial skeletons are preserved for one specimen of *Andrewsiphius sloani* (IITR-SB 2871) and one of *Kutchicetus minimus* (IITR-SB 2647, the holotype); Appendix 1 lists all identified materials for these two specimens. Individual elements for both of these specimens are indicated using numbers behind the decimal point: for instance, the tenth caudal vertebra of the *Kutchicetus* specimen is identified as IITR-SB 2647.201 for easy reference in publication. Measurements for vertebrae and other postcranial elements are summarized in Tables 1 and 2 respectively. The exact vertebral formula is not known for *Kutchicetus* and *Andrewsiphius*, so vertebral positions mentioned herein are estimates.

Cervical vertebrae.—Three centra of cervical vertebrae are preserved for *Kutchicetus* (Fig. 8.5). All three vertebrae of *Kutchicetus* display somewhat triangular facets on cranial and caudal centrum. There are also pronounced sagittal tubercles on the caudal side of the ventral aspect, decreasing in size from IITR-SB 2647.7 to IITR-SB 2647.3, and to IITR-SB 2647.71. These tubercles are presumably for attachment of the longus colli muscle. The transverse canal is preserved in IITR-SB 2647.3 and 2647.71 and is located on the lateral side of the centrum. Parts of the neural canal are preserved in IITR-SB 2647.71 (Fig. 8.5), the maximum width of this canal is 13.7 mm.

Two cervical vertebrae are well preserved for *Andrewsiphius* (Fig. 8.1–4). The centra of *Andrewsiphius* are more rounded than those of *Kutchicetus*. A fragment of the centrum of another cervical vertebra (IITR-SB 2871.6) is more triangular. The sagittal tubercles of IITR-SB 2871.1 and .2 are weaker than in *Kutchicetus*. The size of the longus colli tubercle was probably smaller in more caudal vertebrae and is the basis for our identification of these vertebrae as cervical vertebrae 6 and 7. The neural canal is larger in IITR-SB 2871.2 than in 2871.1 (width: 21.8 mm; height: 14.7 mm). Caudal articular facets are preserved in IITR-SB 2871.2 and face mostly ventral and somewhat lateral.

Thoracic vertebrae.—The anterior thoracic vertebrae of *Kutchicetus* (IITR-SB 2647.1 and 2) are distinct in having a wide centrum (Fig. 8.7) and in being shorter than the cervical vertebrae. Prominent costal facets indent the caudal side of the centrum laterally. The transverse processes project strongly laterally. Middle and posterior thoracic vertebrae (Fig. 8.8–12) have centra that are more or less half-circle-shape in anterior view, increasing in size caudally (Fig. 13). Posterior costal facets are more prominent than anterior costal facets (IITR-SB 2647.7, Fig. 8.8–10). Neural arches are completely preserved for two specimens (IITR-SB 2647.7 width: 17.7 mm; height: 10.5 mm; IITR-SB 2647.8 width 16.7 mm; height 10.8 mm). A transverse process is only preserved in one thoracic vertebra (IITR-SB 2647.7). It bears a depression for the tubercular facet of its rib. Anterior articular facets (IITR-SB 2647.7 and 8) face mostly dorsal and somewhat lateral and cranial, and posterior articular facets match these. A spinous process is preserved only in IITR-SB 2647.7 and is not complete; it is directed caudally.

Preserved thoracic vertebrae of *Andrewsiphius* do not differ morphologically from comparable vertebrae of *Kutchicetus*.

TABLE 1—Vertebral dimensions of measured specimens of *Andrewsiphius sloani* (Sahni and Mishra, 1972) and *Kutchicetus minimus* Bajpai and Thewissen, 2000. Ce, cervical; Th, thoracic; Lu, lumbar; Sa, sacral; Ca, caudal.

	Andrewsiphius sloani				*Kutchicetus minimus*			
	IITR-SB 2871				IITR-SB 2647			
Element	Specimen Number	Length, mm	Width, mm (anterior)	Height, mm (anterior)	Specimen Number	Length, mm	Width, mm (anterior)	Height, mm (anterior)
Ce4					2647.701			30
Ce5					2647.71	24.6	29.6	28
Ce6	2871.1	31.1	33	30.8	2647.3	24.8	26.8	27.3
Ce7	2871.2	34.1	34.3	29.9				
Th1					2647.1	18.4	22.4	17.3
Th2					2647.2	21	22.5	17.2
Th6					2647.72	27.2	28	25.6
Th8					2647.4	26	26.8	27.6
Th9	2871.5	32.4	35.4	30.8	2647.5	25.8	29.3	24
Th10	2871.38	30.4	36.2	27.7	2647.6	26.6	28.8	25.4
Th11					2647.7	26.3	28.6	25.7
Th13	2871.4				2647.8	25.5	28.6	24.1
Lu1					2647.9		36.7	29
Lu3	2871.301	32.2						
Lu4	2871.36	33.8						
Lu5	2871.25	36.5		29.3	2647.101	37.8	47.2	27
Lu6					2647.11	40.4	50.6	28.3
Lu8	2871.8	44.6	42.9	30.1	2647.12		44.1	26.2
Sa1					2647.13	38.4	47.2	25.1
Sa2					2647.13	33.4	31.1	21.3
Sa3					2647.13	33.4	30.6	20.8
Sa4	2871.39	44.5	42.2	29.2	2647.13	32.5	31.8	20.3
Ca1					2647.14	45	32.9	27.6
Ca2					2647.15		38.7	26.7
Ca3					2647.16	45.4	39.8	27.7
Ca5					2647.17	46.6	35.8	29.4
Ca6					2647.18	50.7	37.1	31
Ca8	2871.7	65.6	42.5					
Ca9	2871.3	64	47		2647.19	53.3	34.1	29.3
Ca10	2871.16	62.4	45.4		2647.201	53.5	36.2	30.7
Ca11					2647.21	56.2	33.2	29.6
Ca12					2647.22	55.4	36.4	28.1
Ca14	2871.28		35.3		2647.23	55.4	32.1	26.9
Ca15					2647.24	52.4	33.5	25.5
Ca18	2871.12	58.7	28.3		2647.25		20.3	20.3
Ca19	2871.11	52.4	24.8		2647.26		24	20

Only one of these preserves the neural canal (IITR-SB 2871.38, width: 17.5 mm; height: 13.4 mm; Fig. 8.6). Spinous processes of *Andrewsiphius* were long and robust, as evidenced by a preserved isolated process (IITR-SB 2871.14). This is suggestive of a strong ligamentum nuchae, consistent with the large nuchal crests of the skull.

Lumbar Vertebrae.—Only centra are preserved for lumbar vertebrae of *Kutchicetus* (Fig. 8.13) and *Andrewsiphius* (Fig. 8.14). These centra are similar in that they are wide (Fig. 13) and have broad neural canals. The articular surfaces of these centra are higher and wider than the areas in between these surfaces, giving these vertebrae an hourglass shape. Neural canals are wide (IITR-SB 2647.12, width: 30 mm; IITR-SB 2871.8, width: 25.5 mm), and the root of the transverse process extends along most of the length of the centrum.

Sacrum.—The complete sacrum is known for *Kutchicetus* (IITR-SB 2647.13; Fig. 12.1–3) and a single sacral vertebra is known for *Andrewsiphius kutchensis* (IITR-SB 2871.39). The sacrum of *Kutchicetus* consists of four synostosed vertebrae. IITR-SB 2647.13 was apparently a juvenile individual: synostosis had occurred, but the joints were weak and the

TABLE 2—Limb dimensions of measured specimens of *Andrewsiphius sloani* (Sahni and Mishra, 1972) and *Kutchicetus minimus* Bajpai and Thewissen, 2000.

	Andrewsiphius sloani		*Kutchicetus minimus*	
	IITR-SB 2871		IITR-SB 2647	
Element	Specimen Number	Dimension, mm	Specimen Number	Dimension, mm
Humerus, length	2871.18 and .21	153	2647.401 and .42	140
Humerus, proximal width (med-lat)	2871.18 and .21	47	2647.401 and .42	41
Humerus, distal width (med-lat)	2871.18 and .21	42	2647.401 and .42	39
Radius, proximal width			2647.52	20
Radius, proximal depth (ant-post)			2647.52	12
Femur, length	2871.15 (estim.)	163	2647.41 and .501	131
Femur, proximal width	2871.15	55	2647.41	50
Femur, distal width			2647.501	38
Tibia, length			2647.43 and .44	152
Tibia, proximal width			2647.43	36
Tibia, proximal depth (ant-post)			2647.43	32
Tibia, distal width			2647.44	25

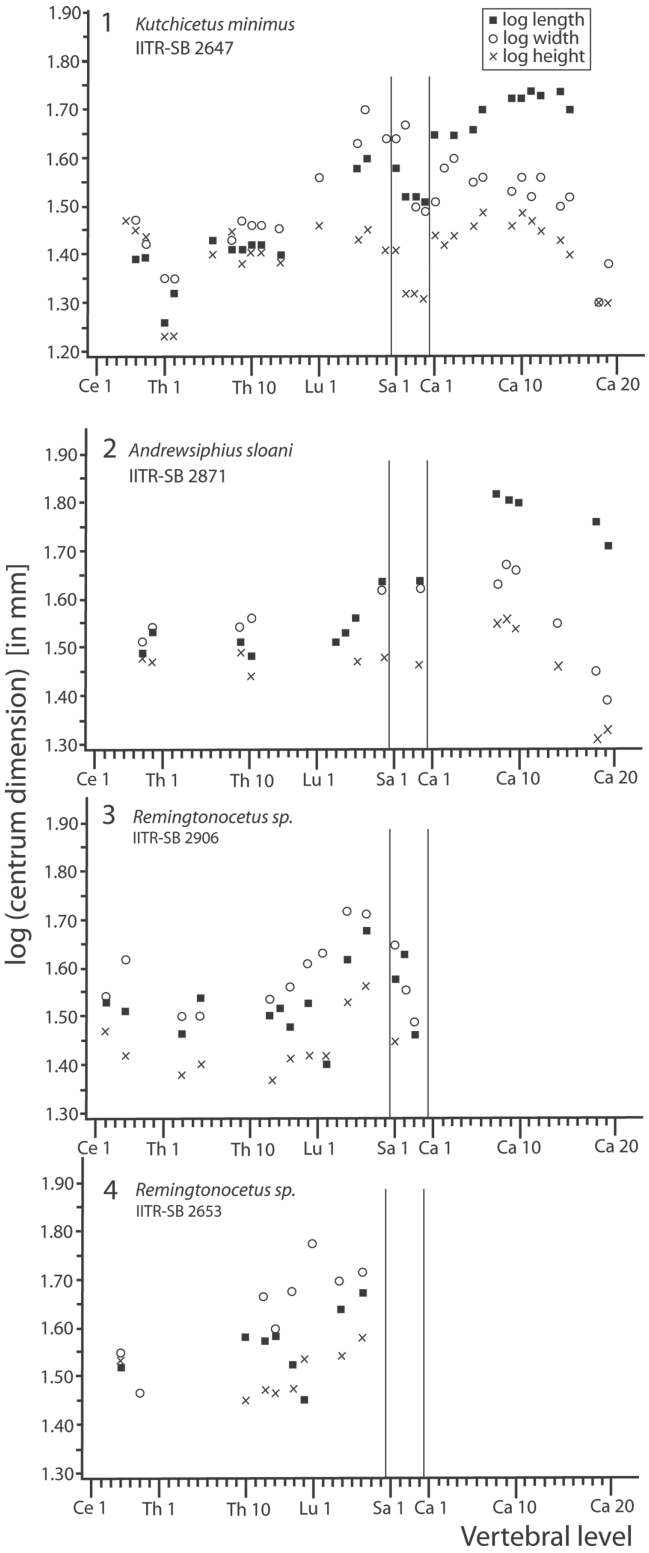

FIGURE 13—Dimensions of the vertebral centra of *1*, *Kutchicetus*; 2, *Andrewsiphius*; and *3*, *4*, two specimens of *Remingtonocetus*. Each plot represents a single individual. Y-axis shows the $\log_{10}$ of centrum length, width, and height in mm. Sacrum position is delineated in plot as it represents a stable part in the vertebral column and is easily identified because its centra are synostosed.

four vertebrae were separated after death and broke at the intervertebral surfaces, although the epiphyses of S1 and S4 were synostosed firmly. Ventrally, bilateral processes reminiscent of hemal processes occur on the junction of S1–S2, S2–S3, S3–S4, as well as on the caudal edge of S4. No such processes occur on the cranial edge of S1. The root of the sacro-iliac joint is preserved on the left side and extends from the cranial part of the body of S1 to the caudal part of the body of S2. This process is thick (dorsoventrally) cranially, and thin caudally. Transverse processes of S3 and S4 are not preserved, but their roots indicate that the process of S4 was thicker than that of S3. The cranial articular processes of S1 are large and slightly concave. They present a broad articulation with the caudal articular processes of the last lumbar vertebra. Articular processes are preserved partly on S1–S2 and S2–S3, but not on S3–S4. Neural arches are preserved for S1–S3, and the roots of the spinous processes are long (craniocaudally) and thick (mediolaterally), suggesting that these processes were high. It is possible that the spinous processes of the sacral vertebrae were fused into a single crest.

The sacral vertebra of *Andrewsiphius* (IITR-SB 2871.39) lacks a vertebral epiphysis, but its articular surface implies that it is either the first or last sacral vertebra. Its dimensions are most consistent with the dimensions of the first sacral vertebra of *Kutchicetus*, but its transverse process is thin dorsoventrally, leaving no space for the auricular surface of the sacro-iliac joint. This indicates that it is a fourth sacral vertebra, and implies that the proportions of the tails of *Andrewsiphius* and *Kutchicetus* are different.

Caudal vertebrae.—The caudal vertebrae of *Kutchicetus* can be divided into three morphological groups, whose morphology suggests that they are from the anterior, central, and terminal sections of the tail as in other Eocene cetaceans (Buchholtz, 1998; Uhen, 2004). For *Andrewsiphius*, preserved caudal vertebrae pertain to the central and terminal segments of the tail.

Five caudal vertebrae, 1, 2, 3, 5, and 6, are preserved from the cranial segment of the *Kutchicetus* tail (Fig. 12.4–6). These vertebrae are short with squat centra, pronounced hemal processes on cranial and caudal rims, and mediolaterally short but craniocaudally long transverse processes. The neural canal is narrow. IITR-SB 2647.17 preserves a relatively complete neural arch. It has a small, flat, oval caudal articular process and the root for a small, but thick spinous process.

The central segment of the tail of *Kutchicetus* is represented by six complete centra, caudal vertebra 9, 10, 11, 12, 14, and 15 (Fig. 9.1–6). These vertebrae have long centra that are wider than long and wider than high (Fig. 13). Hemal processes are present on the rims of the cranial and caudal epiphyses. The pedicles are near the central part of the vertebra in more anterior vertebrae (IITR-SB 2647.19), but are limited to the cranial part of the vertebra in more distal centra. The neural canal is narrow, approximately 5 mm in IITR-SB 2647.23 and 24.

Four vertebrae from the central segment of the tail of *Andrewsiphius* are known (Caudal vertebrae 8 to 10 and 14, Fig. 9.9–12). These are more robust than corresponding vertebrae of *Kutchicetus*, and their centra have different height/width proportions (Fig. 13), but they are otherwise similar. There are separate cranial and caudal transverse processes in IITR-SB 12871.16, whereas in 2871.7 there is only one, centrally placed, transverse process.

The terminal caudal vertebrae of *Kutchicetus* are represented by two fragmentary specimens and three for *Andrewsiphius* (Fig. 9.13–14). These vertebrae (IITR-SB 2871.11 and 12) are long and slender, retain hemal processes similar in size to anterior and posterior transverse processes, and lack a neural arch.

Appendicular skeleton.—The left humerus of *Kutchicetus* (IITR-SB 2647.401 and 42) and right and left humerus of

Andrewsiphius (IITR-SB 2871.17, 18, 201, and 21) are preserved, with only small shaft fragments missing (Fig. 10.1–4; Table 2). Humeri of the two genera are similar in most respects, but *Andrewsiphius* is approximately 10% larger in linear dimensions. The head is strongly convex proximodistally, and narrow mediolaterally. The greater tubercle rises slightly above the head and makes a rounded arc in lateral view. This crest is extended distally with the tuberosity for teres major, the summit of which is proximal on the humeral shaft. The lesser tubercle is a straight crest set more distally and connected cranially with the deltopectoral crest. The summit of this crest is located near the distal part of the humeral head. The bicipital groove is very narrow in *Kutchicetus* but wide in *Andrewsiphius*. The shaft of the humerus is stout, and curves medially. The condyle of the humerus bears a medial epicondyl but lacks a projecting lateral epicondyle. The trochlea is flat, shallow, and wide, whereas the capitulum is narrow and flat and is barely distinct from the trochlea.

Left and right proximal radius (IITR-SB 2647.52 and 56; Fig. 10.5–6) and the right olecranon are preserved for *Kutchicetus* (IITR-SB 2647.51; Fig. 10.7). The proximal radius shows a wide, slightly concave facet for the condyle of the humerus. On the caudal side, the facet for the ulna extends along the entire width of the proximal radius. The shaft of the radius is at a sharp angle with the articular facet, making the limb deviate laterally when articulated with the humerus. A prominent process occurs on the medial side of the proximal radius, possibly for attachment of biceps. The shaft of the radius of *Kutchicetus* is gracile. The olecranon of the ulna (IITR-SB 2647.51) is narrow and deep (craniocaudally). The proximal part of the semilunar notch is preserved and is extended on the medial side of the olecranon.

Left and right femur of *Kutchicetus* (IITR-SB 2647.41, 501, .54, .57; Fig. 10.8–10) and right femur of *Andrewsiphius* are preserved (IITR-SB 2831.15; Fig. 10.11). The femur of andrewsiphiines is short and stocky. The head of the femur is spherical and the greater trochanter robust, reaching as far proximal as the head. The intertrochanteric fossa is deep, and the lesser trochanter a large, triangular blade. There is no third trochanter. The patellar groove of *Kutchicetus* extends obliquely across the distal part of the femur, whereas that of *Andrewsiphius* is more proximodistally directed. The condyles of the femur are spherical and widely spaced, not compressed mediolaterally.

The complete right tibia of *Kutchicetus* is preserved (IITR-SB 2647.43 and .44; Fig. 10.12) and fragments of the right tibia of *Andrewsiphius* (IITR-SB 2831.35). The tibia is narrow and robust with a weak tibial crest. The condyles are more or less circular in circumference. The lateral condyle is more or less flat, whereas the medial condyle is deeply excavated. Distally, the joint for the talus is square in outline. The joint for the lateral side of the trochlea of the talus is broad and deep, whereas that for the medial side of the trochlea is narrower and shallow. A small tibial fragment for *Andrewsiphius* is preserved; it shows a more strongly developed tibial crest.

The left patella is known for *Andrewsiphius* (IITR-SB 2831.29; Fig. 10.14). Its joint for the femur is asymmetrical, extending far medially and less far laterally. A single phalanx is known for *Kutchicetus* (IITR-SB 2647.53; Fig. 9.14). This bone is weathered but shows a narrow shaft and a flat joint for the bone proximal to it.

Innominate.—Five significant fragments of the innominate of *Kutchicetus* are preserved, covering ilium (IITR-SB 2647.33, .35, .46), and ischium (IITR-SB 2647.32 and .34). Overall, these are similar to *Ambulocetus* (Thewissen et al., 2004). As in *Ambulocetus*, the iliac blade projects rostral to the sacro-iliac joint with a triangular extension (IITR-SB 267.33). The ilium is long and stout (Fig. 10.13), and the sacro-iliac joint is well anterior to the acetabulum (IITR-SB 2647.35). The acetabulum is not preserved, but the area of the innominate where it is located is known and consists of thick bone. The ischium is also stout and long (IITR-SB 2647.32, Fig. 10.13) and ends in a large, flat ischial tuberosity. Dorsally, the tip of the tuberosity is divided into two processes, unlike *Ambulocetus* but similar to *Pakicetus*. Overall, the innominate of *Kutchicetus* consists of thicker bone than that of *Pakicetus* and *Ambulocetus*.

Postcranial Comparisons.—The cervical vertebrae of *Kutchicetus* are relatively long, longer than anterior thoracic vertebrae and similar in length to central thoracic vertebrae. This is not the case in many other early cetaceans, such as *Ambulocetus* (Thewissen et al., 1996), *Rodhocetus*, and *Georgiacetus* (Buchholtz, 1998). In *Remingtonocetus* (IITR-SB 2871, Fig. 13), cervical vertebrae are similar in length to anterior thoracic vertebrae. The height of the cervical vertebrae of *Remingtonocetus* (Fig. 13) is less than in *Kutchicetus* and *Andrewsiphius*.

The anterior thoracic vertebrae of *Kutchicetus* are much wider than they are long or high (Fig. 13), which is unlike *Ambulocetus* (Madar et al., 2002) and protocetids (Buchholtz, 1998). No anterior thoracic vertebrae are known for *Andrewsiphius*. Thoracic vertebra 11 of *Kutchicetus* (IITR-SB 2647.7) has a spinous process that projects caudally more than the spinous processes of the vertebrae of *Ambulocetus* in this area.

There are differences in the relative dimensions of the lumbar vertebrae between *Kutchicetus* and *Andrewsiphius*. In *Kutchicetus*, lumbar vertebrae are significantly longer than thoracic vertebrae, whereas in *Andrewsiphius* thoracic and lumbar vertebrae are similar in length. *Kutchicetus* is unusual among early cetaceans: lumbar vertebrae in *Ambulocetus* and protocetids are more or less similar in length (Buchholtz, 1998; Madar et al., 2002)

Proportional differences in the last sacral vertebra of *Andrewsiphius* and *Kutchicetus* suggest that the cranial part of the tail in the latter was more strongly developed than that of the latter. Centra of the sacrum of *Kutchicetus* are similar in length to those of pakicetids but are clearly broader (H-GSP 96267; Madar, 2007), suggesting that the tail was stronger in *Kutchicetus*. The spinous processes of the sacral vertebrae of *Kutchicetus* are similar to those of pakicetids, and less strongly developed than those of *Ambulocetus* (H-GSP 18507; Madar et al., 2002). In *Remingtonocetus*, the sacrum tapers strongly and the last sacral vertebra is short and narrow (IITR-SB 2906, Fig. 13), unlike that of *Kutchicetus*. It is possible that the tail of *Remingtonocetus* was shorter and less muscular than that of *Andrewsiphius* and *Kutchicetus*. In *Dalanistes*, the last sacral vertebra is narrower, but not shorter than the first sacral vertebra (Gingerich et al., 1995).

Caudal vertebrae of *Kutchicetus* and *Andrewsiphius* are robust, suggestive of muscular tails. Although overall similar to caudal vertebrae of *Ambulocetus* (Madar et al., 2002) and pakicetids (Madar, 2007), they exhibit proportional differences. Height/width ratios of the vertebral body of mid-caudal vertebrae in pakicetids vary from 1.04 to 1.33 (H-GSP 92053, 96366, and 96564) and those of *Ambulocetus* are approximately 0.86–0.92 (H-GSP 18507.811 and .812; Madar et al., 2002), whereas in *Dorudon*, these ratios are between 0.8 and 0.9 (Uhen, 2004). In *Kutchicetus*, this ratio varies from 0.76 to 0.89 (IITR-SB 2647, presumed Ca 9–12), and in *Andrewsiphius*

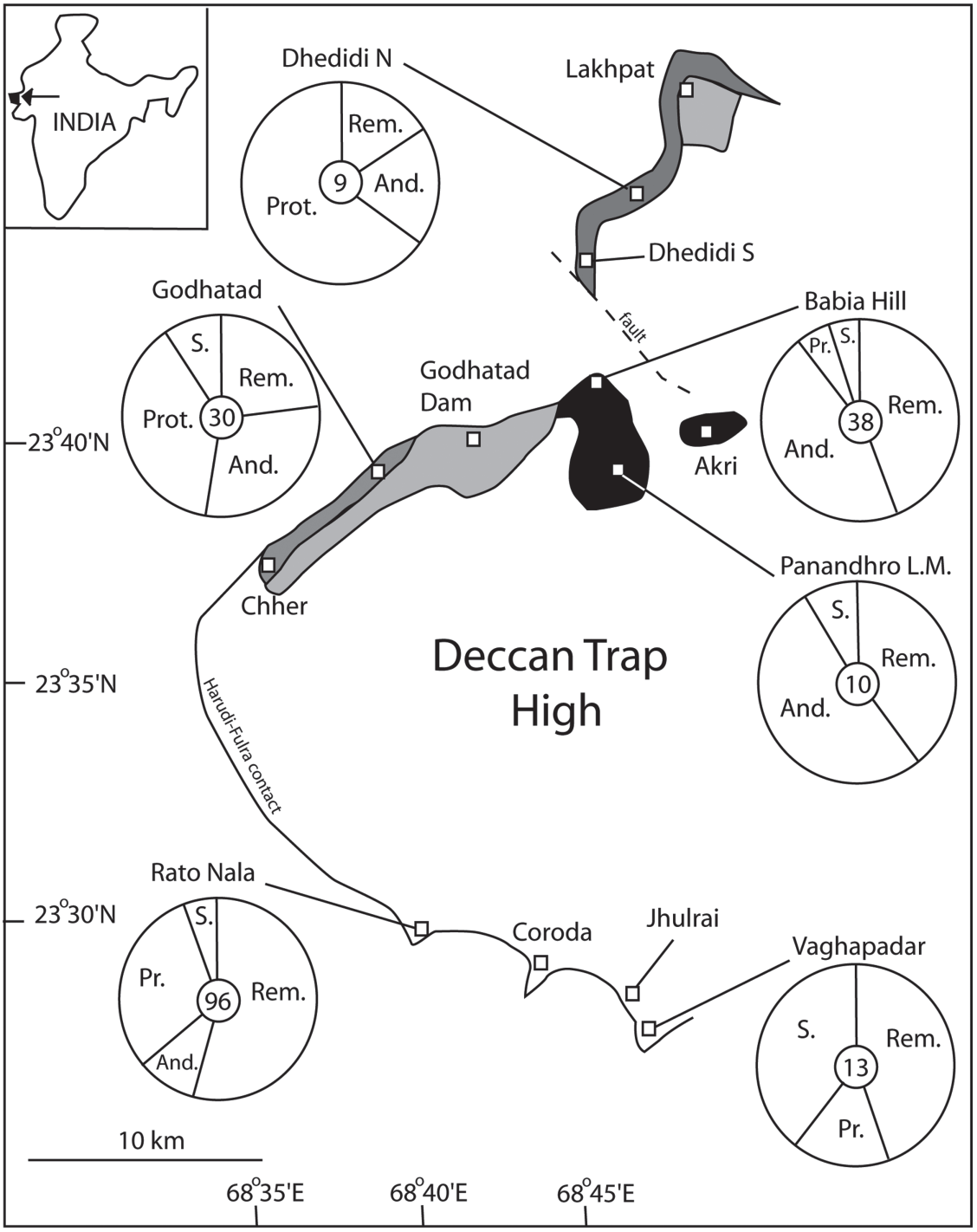

	Saraswati & Banerjee, 1984	Mukhopadhyay & Shome, 1996	Biswas, 1992
Bartonian	Fulra Fm.	Fulra Fm.	Fulra Fm.
Lutetian	Harudi Fm.	Harudi Fm.	Harudi Fm.
	Panandhro Fm.	Lakhpat Fm.	Naredi Fm.

Marsh, swamp
Tidal flat, organic bank
Lagoon

Rem., remingtonocetines
And., andrewsiphiines
Pr., protocetids
S., sirenians

FIGURE *14*—Map of marine mammal fossil localities (white squares) in Kutch, superimposed on inferred sedimentary environments (as determined by Muhkhopadhyay and Shome, 1996). Localities are just below the Harudi-Fulra contact and surround a central dome consisting of Deccan Trap volcanics. Rose diagrams indicate relative abundance of several marine mammal groups based on unambiguously identifiable specimens (sample size in

from 0.75 to 0.83 (IITR-SB 2871, presumed Ca 8–10). These values should be interpreted with caution, as the exact position of all of these specimens in the vertebral series is not known, but there is a clear suggestion that the mid-caudal vertebrae of *Kutchicetus* and *Andrewsiphius* are flattened with respect to the other archaeocetes. Vertebrae from the central part of the tail in *Lutra* and *Enhydra*, swimmers with rounded tails, have similar values for height and width (Buchholtz, 1998). These data are consistent with the interpretation that the tails of *Kutchicetus* and *Andrewsiphius* are flattened. The shape of the tail vertebrae further suggests that there was no fluke in *Andrewsiphius* and *Kutchicetus* (Bajpai and Thewissen, 2000). Long bones of *Kutchicetus* and *Andrewsiphius* show that these animals had short and stout extremities, as is common in swimmers. Since only a few hand- and foot-ones are known, the size of the autopodium cannot be determined.

Locomotion.—Thewissen and Fish (1997) proposed a model of cetacean locomotor evolution based on studying modern lutrines, which suggested that *Ambulocetus* swam using pelvic paddling with additional lift provided by dorsoventral undulations of the tail. Buchholtz discussed the relation between swimming modes and vertebral column morphology in Oligocene to modern cetaceans (2001) and in Eocene whales (1998). She proposed (1998) that *Ambulocetus* and *Remingtonocetus* swam by undulating their lumbar vertebral column, which powered their feet, consistent with the findings of Thewissen and Fish (1997), whereas in protocetids, the tail has a more significant propelling surface. Madar et al. (2002) also found that aquatic locomotion in *Ambulocetus* employed mostly the foot as its hydrofoil. Bajpai and Thewissen (2000) proposed that the vertebral dimensions of *Kutchicetus* are unlike those of previously studied cetaceans and that it propelled itself using the tail as a hydrofoil. Such a swimming mode is similar to that of the otter *Pteronura*, which has a long, dorsoventrally flattened tail. Proportions of the caudal vertebrae of *Kutchicetus* and *Andrewsiphius* are consistent with this as shown by Bajpai and Thewissen (2000). This hypothesis also coincides with the cetacean locomotor evolution model of Thewissen and Fish (1997). In fact, that model predicted morphologies such as those of *Kutchicetus* (Thewissen and Williams, 2001) and lends support for the view that modern otters are an excellent model for swimming morphology of Eocene whales. It appears then that andrewsiphiines use their tails to propel themselves in water as do modern whales.

The innominate of *Kutchicetus* is similar to that of other early cetaceans, in particular pakicetids (Madar, 2007) and *Ambulocetus* (Thewissen et al., 1996). All three taxa are characterized by large ischial tuberosities, the area where the adductors of the thigh would attach. The femur in these animals is short, and matches the (estimated) distance between acetabulum and ischial tuberosity. Therefore, adductor muscles extending between the ischial tuberosity and proximal tibia would have run mostly mediolaterally and would have functioned most efficiently as adductors (unlike many mammalian quadrupeds, where they are important dorsiflexors of the hip).

No trace of the pubic symphysis remains in *Kutchicetus*. The pubic symphysis of *Pakicetus* and *Ambulocetus* is small and rounded and restricted to the cranial portion of the interpubic region. Hulbert (1998) described a short pubic symphysis in *Georgiacetus*. The small size of the pubic symphysis in these early whales is also consistent with poorly developed land locomotion. Marine mammals with hind limbs (e.g., phocids) have a small pubic symphysis, presumably reflecting the absence of strong forces abducting the innominate caused by weight-bearing and adducted hind limbs.

DEPOSITIONAL ENVIRONMENT

The localities where fossil cetaceans have been found in Kutch occur in a crescentic belt of Tertiary rocks around an outcrop of Deccan Traps, K-T boundary aged volcanic deposits (Fig. 14). Structurally this represents a dome, with Deccan basalts in the center and anticlinal rings of younger rocks. In the Eocene, there was a coastal plain to the south of the Traps, toward the Arabian Sea. To the west and north were more protected marginally marine environments. The modern topography is not very different; to the west and north of modern Kutch are the salt flats of the Rann of Kutch, which flood during Monsoon time. The Eocene represents a transgressive sequence with several cycles of sea level change and is traditionally divided into the Naredi, Harudi, and Fulra Formations (following Biswas, 1992). Given the distinct lithological differences between the type section of the Naredi Formation (south of the Deccan Traps and devoid of mammalian fossils) and the beds underlying the Harudi Formation to the north and west of the Deccan outcrops (with marine mammal fossils), we refer to these latter beds as the Panandhro Formation, following Saraswati and Banerjee (1984). A detailed sedimentological study of these western and northern pre-Fulra outcrops was undertaken by Mukhopadhyay and Shome (1996), who were specifically interested in the depositional environment of the commercially important lignites of the Panandhro Formation in outcrop and subcrop. This study forms the basis for our interpretations of sedimentary environments, as also previously discussed by Bajpai et al. (2006).

Cetacean and sirenian specimens that are identifiable at the genus level were tallied at our six richest localities. At these localities, total abundance of remingtonocetines, andrewsiphiines, protocetids, and sirenians varied from 9 to 96 specimens, and the relative abundance of these groups is presented in rose diagrams in Figure 14. The localities Dhedidi North and Godhatad are characterized by a high percentage of protocetids, while among remingtonocetids, andrewsiphiines and remingtonocetines are equally abundant. Sirenians are rare at these localities. Godhatad and Dhedidi North were interpreted as a tidal and lagoonal lithofacies by Mukhopadhyay and Shome (1996). Protocetids are nearly absent, sirenians are rare, and remingtonocetines and andrewsiphiines are approximately equally abundant at the localities Babia Hill and Panandhro Lignite Mine. The depositional environment at these localities was interpreted as marsh or swamps by

←

center of rose) in six localities. Southern localities face the Indian Ocean, northern localities face the Rann of Kachchh. These rocks have been classified into different formations by different authors as indicated in the table below. A similar map with more modern topographical landmarks for this area was published by Bajpai and Thewissen (2006). Coordinates and topography are taken from unofficial or ancient maps of this area. Kutch is on a sensitive national border, and there are no guarantees that coordinates, such as those acquired using GPS, are accurate. Individuals interested in acquiring coordinates should contact the authors.

TABLE 3—Complete character state scores for Pakicetidae, *Remingtonocetus*, *Andrewsiphius*, and *Kutchicetus*.

Pakicetidae	10?010??00 ?00(01)(01)010?0 1120010311 0001111101 11?0100110 1101001001 0121100111 1001011111 000?0?0?0? ?00301?01? ??00000000 ?0000
Remingtonocetus	112(12)12?011 3110100100 11(02)00121?? 20?1????11 11?01111?? 10020130?1 ?121112202 20022(23)(23)2(23)3 1?00100??? 0?0301???? ???????010 0011?
Andrewsiphius	112001??23 3310201100 ???20?1031? 00?0?110?? 0???111?01 ?1?2013101 01?1?01101 200023(23)1(23)4 110??????? ?????????? ???????101 11?12
Kutchicetus	11?001??23 3310?0110? ???0??01?? 0???0?110?? ?????????? ?1?20131?0 ???1?01101 ???023(23)1(23)4 110?1?0?0? 21030?00?? ??001?01?? 11??2

Mukhopadhyay and Shome (1996). Unlike protocetids, *Remingtonocetus* had small eyes (Thewissen and Nummela, 2008), consistent with the muddy water that could be expected in swamps and marshes.

The faunal composition at these northern and western localities is distinctly different from those to the south of the Deccan Traps, an area not studied by Mukhopadhyay and Shome (1996). Our richest southern locality, Rato Nala, bears most fossils in a lithology called the Chocolate Limestone, a muddy, nodular limestone with many burrows and closed bivalve shells. This limestone is not found at other localities and is suggestive of a productive but muddy shallow sea. Rato Nala has abundant protocetids and remingtonocetines but few andrewsiphiines and sirenians. The most unusual locality is Vaghapadar, where sirenians dominate the fauna. This locality may represent a fossil seagrass bed (Bajpai et al., 2006).

Matching sedimentary studies and marine mammal abundance data, it appears that the middle Eocene cetaceans of Kutch had clear habitat preferences, with protocetids more abundant in clearer, more open water settings, and andrewsiphiines most common in swamps and marshes. Remingtonocetines were abundant everywhere, and all taxa are found in the intertidal environments.

PHYLOGENETIC ANALYSIS

In order to determine the relationship of *Andrewsiphius* and *Kutchicetus* to other Eocene cetaceans, we executed a phylogenetic analysis. Many authors have studied Eocene cetaceans phylogenetically (e.g., Thewissen, 1994; Geisler and Luo, 1998; Hulbert et al., 1998; Luckett and Hong, 1998; O'Leary, 1998; Uhen, 1998; O'Leary and Geisler, 1999; Thewissen and Hussain, 2000; Geisler, 2001; Thewissen et al., 2001, 2007; Geisler and Uhen, 2003; Geisler et al., 2005, 2007; O'Leary and Gatesy, 2007). The basis for our analysis is the study published by Geisler (2005), who compiled most characters used by previous authors and provided detailed, well-referenced descriptions in an analysis that included many early cetaceans as well as some artiodactyls and mesonychians.

Complete skeletons are not known for either *Andrewsiphius* or *Kutchicetus*. Scores for these taxa are based by combining observations made on multiple specimens, a common practice in vertebrate paleontology although occasionally questioned by non-specialists. *Andrewsiphius* scores are based on 11 specimens. Nine of these specimens include material that unambiguously identifies them as *Andrewsiphius*: the narrow, high maxilla widening only slightly near the molars, and the mandible with the long, fused symphysis. These are highly unusual features in a mammal, and it is unlikely that *Andrewsiphius* is confused with any other taxon. The two specimens that do not include such diagnostic gnatic material (IITR-SB 2534 and 2879) were used to score character state 2 for Character 28, making its score polymorphous for *Andrewsiphius* (the state 28:3 is based on IITR-SB 2517, a specimen that includes gnatic material).

All scores for the phylogenetic analysis of *Kutchicetus* are based on four specimens: IITR-SB 2636, 2647, 2791, and VPL 1007. IITR-SB 2647 is the holotype and includes a small maxillary fragment that shows the unique feature of this species: the extreme narrow maxilla in which the palate flares lingually between subsequent teeth in the incisor/canine area. This feature can be used to identify IITR-SB 2791 and VPL 1007 unambiguously to *Kutchicetus*. IITR-SB 2636 is a mandible which occludes well with VPL 1007, displays the same narrow morphology, and is distinctly different from *Andrewsiphius* lower jaws. Moreover, IITR-SB 2636 matches the shape of an impression with bone fragments that is part of the holotype.

We have adapted the analysis by Geisler et al. (2005) to incorporate the morphological variation observed in our sample. We have also deleted the non-cetacean taxa from the analysis, as these are outside the scope of the present study. As a result, some of characters of the analysis by Geisler et al. (2005) are uninformative. We ran two analyses; in the first we followed the views of Geisler et al. (2005) in which characters are ordered (3, 4, 5, 6, 7, 8, 10, 11, 14, 16, 20, 26, 28, 33, 54, 58, 60, 62, 63, 67, 71, 76, 77, 78, 79, 80, 88, 90, 91, 92, 93, 94, and 115), whereas in the second analysis all characters were considered unordered. We then reran the analysis deleting character state 28:2 for *Andrewsiphius*, as this state was based on material that could not be attributed to this taxon beyond any doubt.

We chose Pakicetidae as the outgroup for both analyses, using the scores of Geisler et al. (2005) for this clade. Table 3 and Appendix 2 present the scores for *Andrewsiphius* and *Kutchicetus* for the characters in the study of Geisler et al. (2005), using their numbering system. Table 3 and Appendix 2 also show which characters for the clades Pakicetidae and *Remingtonocetus* are scored differently by us than by Geisler et al. (2005). Appendix 3 discusses scores for the new characters for all studied taxa. In addition, we added new characters to the analysis (108 to 115). Here, we will discuss only those characters which were modified from the analysis of Geisler et al. (2005).

Character 3.—The length of the reconstructed skull of *Andrewsiphius*, based on IITR-SB 2517, 2751, and 2907, is 770 mm and its condylar width 60 mm. The score for *Andrewsiphius* is thus 2.

Characters 9 to 11.—Characters 9 to 11 of the Geisler et al. (2005) analysis relate to the presence of embrasure pits. Embrasure pits in the palate are depressions which receive the tips of the lower teeth when the mouth is closed (Thewissen, 1994). In *Andrewsiphius* and *Kutchicetus*, the lower dentition is lodged in indentations in the maxilla, but, given the extreme narrowing of the jaw, these indentations indent the jaw more laterally than ventrally and are thus dissimilar to the embrasure pits of other Eocene cetaceans. This requires adding a new state to accommodate this condition. For character 9, this is state 2, and for Character 10, it is state 3.

Character 11 already had a state describing this condition in the study of Geisler et al. (2005).

Character 13.—Rostrum breadth in Pakicetidae is 144% of bicondylar width and thus scored as 0 (H-GSP 18470 and 96231).

Character 14.—This character describes how far the caudal palatine notch indents the posterior palate.

Character 17.—Orbital size in Pakicetidae is well over 30% of bicondylar width, hence scored as 1 (H-GSP 96231)

Character 27.—In *Andrewsiphius* (IITR-SB 3153), there is a rugose, elevated area for attachment of one of the neck muscles on the base of the basioccipital, and the anterior part of it does attach to the tympanic. Such a tubercle is also present in pakicetids (Nummela et al., 2006). This process differs from the falcate process of later whales and is dissimilar to the laterally projecting falcate process of *Remingtonocetus*, which was correctly described as autapomorphic by Geisler et al. (2005).

Character 28.—This character of Geisler et al. (2005) expressed the length of the external auditory meatus as a function of basicranial width. We determined this value for three specimens of *Andrewsiphius*, IITR-SB 2534, 2879, 3153, and one of *Kutchicetus*, VPL 1007. The ratio used by Geisler et al. (2005) for these specimens is, respectively: 0.41, 0.42, 0.32, and 0.24, resulting in scores of 2 and 3 for *Andrewsiphius* and 1 for *Kutchicetus*.

Character 55.—The sigmoid process of *Andrewsiphius* points dorsally more than being a transverse plate, and is similar in this respect to *Remingtonocetus*.

Character 57.—The median furrow of the tympanic in *Andrewsiphius* is similar to that of *Gaviacetus*, which was scored as 3 by Geisler et al. (2005).

Character 55.—*Remingtonocetus* is rescored as 0 (IITR-SB 2828; VPL 1004).

Character 62.—Pakicetids are rescored as 1 (Nummela et al., 2006).

Character 66.—*Remingtonocetus* is rescored as 1 (IITR-SB 2592)

Character 67.—*Remingtonocetus* has accessory cusps in its premolars and lower molars, similar to basilosaurids, and is scored 2 (IITR 2650).

Character 70.—In pakicetids, p4 and p3 are similar in length; the length ratio p4/p3 is around 1.0 to 1.1 (GSP-UM 1981; H-GSP 91036). In *Remingtonocetus*, the length ratio p4/p3 is 0.75 (IITR-SB 2521). In *Andrewsiphius* (IITR-SB 2723) this ratio is 0.92. These teeth are not known for *Kutchicetus*, but its single-rooted p3 is certainly much shorter than its p4.

Character 73.—*Andrewsiphius* and *Kutchicetus* lack a reentrant groove and are scored as 0. Geisler et al. (2005) perceived this state to imply the anterior side of the trigonid to be flat; however, in this case it is slightly convex. *Remingtonocetus* is rescored as 0.

Character 74.—In taxa in which the lower molars bear a number of cusps decreasing in size from anterior to posterior, only the first of these is considered the trigonid (Geisler, pers. comm., 2007). We here recharacterize the scores to accurately reflect the condition in *Andrewsiphius*, where the trigonid is much longer than the talonid. As such, pakicetids, ambulocetids, and protocetids are scored 1: trigonid and talonid similar in length (scored as 0 by Geisler et al., 2005). *Remingtonocetus*, *Basilosaurus*, and *Dorudon* are scored 2: talonid longer than trigonid (Geisler et al.'s 1). *Andrewsiphius* is scored 0: trigonid longer than talonid. This is an ordered character.

Character 80.—The mandibular symphysis of *Remingtonocetus* usually ends at P3, not P4 (IITR-SB 2704); the taxon is rescored as 3.

Character 81.—As described above, the mandibular symphysis in *Remingtonocetus* is usually unfused (e.g., IITR-SB 2704).

Character 91.—This character should be scored using the longest vertebra in the lumbosacral range (Geisler, pers. com., 2007) and compares its length to the length of the first thoracic vertebra.

Character 108.—Lower p4 more than 10% longer than m1 (0) or similar/shorter than m1 (1).

Character 109.—Lower molars with distinct trigonid and talonid, each with one dominant cusp (0) or distinction between trigonid and talonid blurred by the insertion of additional cusps posterior to protoconid (1).

Character 110.—Paracone somewhat higher than metacone on M2, but both cusps clearly distinct (0), metacone reduced to small cuspule on postparacrista (1).

Character 111.—Snout width (left plus right medio-laterally) more then 80% of dorso-ventral height (0) at posterior M2, or less than 80% (1), causing the palate to be narrow even at the molars.

Character 112.—Paroccipital process straight (0) or strongly curved and pointing anteriorly (1).

Character 113.—Cerebellar endocast (or endocast of cerebellar rete) lower (0) or higher (1) than cerebral endocast.

Character 114.—Height of coronoid process more than 1.5 times as high as the dentary at m3 (0) or less than 1.5 times as high as dentary (1).

Character 115.—Shape of mid caudal vertebrae (near Ca6). Average centrum height/width above 1.00 (0), between 0.85 and 1.00 (1), or below 0.85 (2). This character is ordered.

Both analyses included all cetaceans in the study by Geisler et al. (2005) with the addition of *Andrewsiphius* and *Kutchicetus* and used the branch-and-bound algorithm of PAUP version 4.0b10 (Swofford, 2002). The analysis with ordered characters yielded five most parsimonious trees, and the analysis with all characters unordered yielded three. In all trees of both analyses, *Andrewsiphius* and *Kutchicetus* are sister taxa, here considered Andrewsiphiinae.

Comparison of the five trees in the analysis with ordered characters shows that *Dalanistes* occupies different positions in the tree. The analysis was redone after deletion of *Dalanistes*. All analyses (ordered/unordered, with/without *Dalanistes*) were run again, now with Character 28:3, as opposed to 28(2,3) for *Andrewsiphius*. This did not affect the topologies for any of the trees.

In the consensus cladogram of the analysis with only unordered characters, Andrewsiphiinae (*Andrewsiphius* and *Kutchicetus*) and Remingtonocetinae (*Remingtonocetus* and *Dalanistes*) are both monophyletic. The node at their base shows andrewsiphiines and remingtonocetines sometimes as successive branches on the cetacean tree, sometimes as a monophyletic family Remingtonocetidae (with Andrewsiphiinae and Remingtonocetinae as subfamilies).

The five most parsimonious trees (of the analysis that has Character 28(2,3) for *Andrewsiphius*) are 298 steps in length, have a consistency index of 0.700 (excluding uninformative characters) and a retention index of 0.713. Character changes supporting Andrewsiphiinae in all five trees are 4, 5, 9, 10 (to state 2), 12, 15, 41, 80, 108, 110, 111, and 112. As stated, deletion of *Dalanistes* in this analysis results in two most

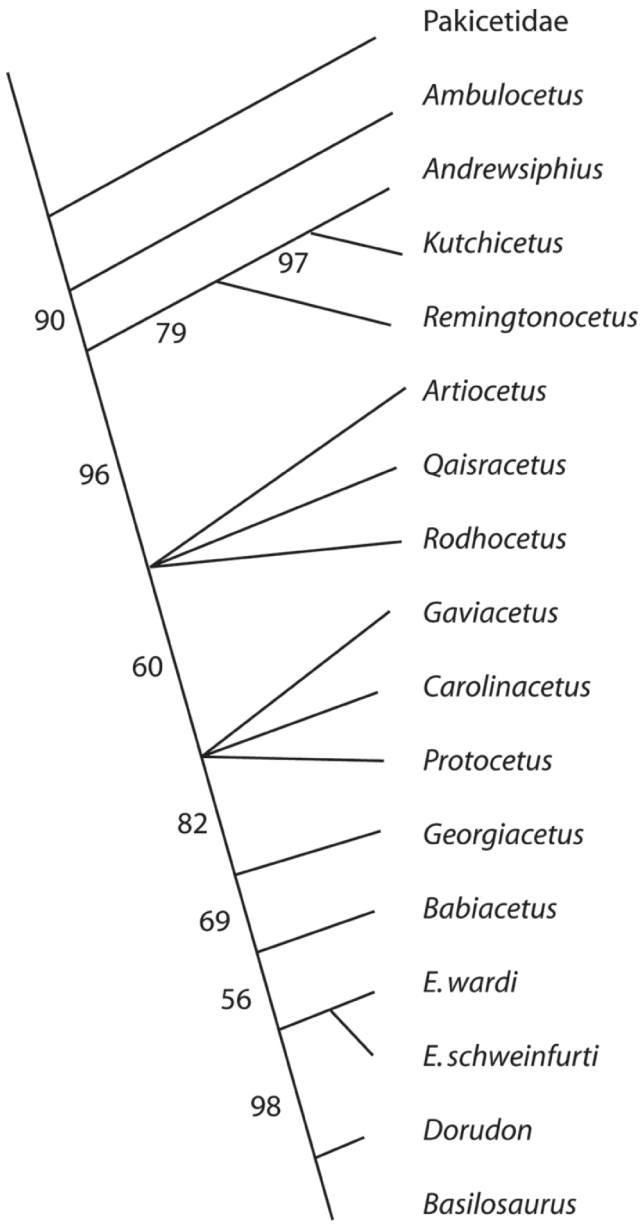

FIGURE *15*—Bootstrap 50% majority rule consensus phylogeny of early cetaceans, with Pakicetidae as outgroup, and some characters ordered (see text). Numbers are bootstrap values. Character analysis and scores of Geisler (2005), with some modifications as described in the text. The genus name *Eocetus* is abbreviated as *E.*

parsimonious trees that both show monophyletic *Remingtonocetus* plus Andrewsiphiinae.

Consensus cladograms for the eight analyses differ regarding the monophyly of remingtonocetines (*Remingtonocetus* and *Dalanistes*) and remingtonocetids (remingtonocetines and andrewsiphiines), and the phylogeny of protocetids. All eight analyses (unordered characters versus ordered/unordered characters; inclusion or exclusion of *Dalanistes*; Character 28 polymorphic for *Andrewsiphius* or not) agree on the monophyly of andrewsiphiines, and the position of remingtonocetines and andrewsiphiines as between *Ambulocetus* and the protocetids on the cetacean cladogram. The bootstrap 50% majority rule consensus cladogram for the analysis excluding *Dalanistes* and with all unordered characters is shown in Figure 15. A detailed study of the Remingtonocetinae (*Remingtonocetus* and *Dalanistes*) is necessary to resolve the exact phylogenetic position of this taxon (which may not be a clade), and at this point we prefer the conservative interpretation of including *Andrewsiphius* and *Kutchicetus* as a subfamily of Remingtonocetidae.

CONCLUSIONS

Andrewsiphius sloani and *Kutchicetus minimus* are a monophyletic group of Eocene cetaceans, clearly distinct morphologically from each other, but also clearly closely related because they share unusual synapomorphies. *Andrewsiphius* and *Kutchicetus* are mostly known from the Lutetian (42–46 m.y.a.) of Kutch, India. The depositional environments of the Indian localities included nearshore marine bays and swamps (Mukhopadahyay and Shome, 1996). *Andrewsiphius* and *Kutchicetus* have highly unusual skulls, with long and narrow rostra, that nevertheless were relatively high dorsoventrally. Their molars played a minor role in food processing, but more anterior teeth were significant. The large sagittal crest indicates that the chewing muscles were large, but the angle at which these muscles inserted is low, suggesting an unusual, and as yet not understood, feeding mechanism. The eyes are set close to the midline of the skull but are not small (unlike *Remingtonocetus*). Andrewsiphiines probably lived in turbid water, suggesting that the eyes were mainly used in air, possibly at the water's surface when the animal was submerged. Olfaction still played a role as a sense organ, and the morphology of the premaxilla suggests that mechanoreception at the tip of snout was significant. It is possible that andrewsiphiines dug in soft mud to find prey, using mechanosense to locate prey, but it is also possible that they detected eddies of swimming prey using these organs, in a way similar to modern seals (Dehnhardt and Mauck, 2008). Their hearing was partly adapted for underwater sound, and the modern sound receiving mechanism of whales (Nummela et al., 2004, 2007) was present.

Kutchicetus and *Andrewsiphius* had short and stocky limbs, well able to support their weight on land. Their neck was long and mobile, a primitive feature for cetaceans, and their sacrum fused and anchored strongly to the hind limb. In water, *Kutchicetus* and *Andrewsiphius* propelled themselves mostly by means of undulations of the long tail (Bajpai and Thewissen, 2000; Thewissen and Williams, 2002), which was probably flattened dorso-ventrally.

The andrewsiphiines represent one of the lowest branches of the cetacean cladogram, they probably are the sister group to *Remingtonocetus* and together included in Remingtonocetidae, although it remains possible that andrewsiphiines are a basal branch separate from *Remingtonocetus*.

ACKNOWLEDGMENTS

We thank the people involved in collecting the material on which this study was based: B. Armfield, E. Byron, L. Cooper, V. V. Kapur, N. Saravanan, R. Sharma, L. Stevens, and B. N. Tiwari. We thank R. Lupia, editor of this journal, for his patience and diligence during the editorial process, and the reviewers for their insightful comments. We thank the Gujarat Mineral Development Corporation, and especially A. Thakore, for logistic support. We also thank P. H. Bhatti, for help in conducting field work efficiently. Fossils were prepared by B. Armfield, R. Conley, and L. Stevens, and drawings were made by J. Dillard. Grants from the National Science Foundation (Earth Sciences and International Programs) of the USA. to J. G. M. T., and from the Department of Science and Technology of India (including a Ramanna Fellowship) to S. B., funding this work.

REFERENCES

BAJPAI, S. AND J. G. M. THEWISSEN. 1998. Middle Eocene cetaceans from the Harudi and Subathu Formations of India, p. 213–233. *In* J. G. M. Thewissen (ed.), The Emergence of Whales, Evolutionary Patterns in the Origin of Cetacea. Plenum Press, New York, 477 pp.

BAJPAI, S. AND J. G. M. THEWISSEN. 2000. A new diminuitive whale from Kachchh (Gujarat, India) and its implications for locomotor evolution of cetaceans. Current Science (New Delhi), 79:1478–1482.

BAJPAI, S. AND J. G. M. THEWISSEN. 2002. Vertebrate fauna from Panandhro Lignite field (Lower Eocene), District Kachchh, western India. Current Science (New Delhi), 82:507–509.

BAJPAI, S. AND J. G. M. THEWISSEN. 2006. Eocene and Oligocene sirenians (Mammalia) from Kachchh, India. Journal of Vertebrate Paleontology, 26:400–410.

BISWAS, S. K. 1992. Tertiary biostratigraphy of Kutch. Journal of the Palaeontological Society of India, 37:1–29.

BRISSON, M. J. 1762. Regnum animale in classes IX distributum, sive synopsis methodica sistens generalem animalium distributionem in classes IX, & duarum primarum classium, quadripedum scilicet & cetaceorum, particularum divisionem in ordines, sections, genera, & species. Editio altera auctior. Theororum Haak, Leiden (Netherlands), 296 pp.

BUCHHOLTZ, E. A. 1998. Implications of vertebral morphology for locomotor evolution in early Cetacea, p. 325–351. *In* J. G. M. Thewissen (ed.), The Emergence of Whales, Evolutionary Patterns in the Origin of Cetacea. Plenum Press, New York, 477 pp.

BUCHHOLTZ, E. A. 2001. Vertebral osteology and swimming style in living and fossil whales (Order: Cetacea). Journal of Zoology, 253:175–190.

DEHNHARDT, G. AND B. MAUCK. 2008. Mechanoreception in secondarily aquatic vertebrates, p. 295–314. *In* J. G. M. Thewissen and S. Nummela (eds.), Sensory Evolution on the Threshold, Adaptations in Secondarily Aquatic Vertebrates. University of California Press, Berkeley, 360 pp.

FISH, F. E. 1996. Transitions from drag-based to lift-based propulsion in mammalian swimming. American Zoologist, 36:628–641.

FISH, F. E. 2001. A mechanism for evolutionary transition in swimming mode by mammals, p. 261–287. *In* J.-M. Mazin and V. de Buffrénil (eds.), Secondary Adaptations of Tetrapods to Life in Water. Dr. Friedrich Pfeil Verlag, Munich, 367 pp.

GEISLER, J. 2001. New morphological evidence for the phylogeny of Artiodactyla, Cetacea, and Mesonychidae. American Museum Novitates, 3344:1–53.

GEISLER, J. AND Z.-X. LUO. 1998. Relationships of Cetacea to terrestrial ungulates and the evolution of cranial vasculature in Cete, p. 163–212. *In* J. G. M. Thewissen (ed.), The Emergence of Whales, Evolutionary Patterns in the Origin of Cetacea. Plenum Press, New York, 477 pp.

GEISLER, J., A. E. SANDERS, AND Z.-X. LUO. 2005. A new protocetid whale (Cetacea: Archaeoceti) from the late middle Eocene of South Carolina. American Museum Novitates, 3480:1–65.

GEISLER, J. H, J. M. THEODOR, M. D. UHEN, AND S. E. FOSS. 2007. Phylogenetic relationships of cetaceans to terrestrial artiodactyls, p. 19–31. *In* D. R. Prothero and S. E. Foss (eds.), The Evolution of Artiodactyls. Johns Hopkins University Press, Baltimore.

GEISLER, J. AND M. D. UHEN. 2003. Morphological support for a close relationship between hippos and whales. Journal of Vertebrate Paleontology, 23:991–996.

GINGERICH, P. D., M. ARIF, AND W. C. CLYDE. 1995. New archaeocetes (Mammalia, Cetacea) from the middle Eocene Domanda Formation of the Sulaiman Range, Punjab (Pakistan). Contributions from the Museum of Paleontology, University of Michigan, 29:291–330.

GINGERICH, P. D., M. UL-HAQ, I. H. KHAN, AND I. S. ZALMOUT. 2001a. Eocene stratigraphy and archaeocete whales (Mammalia, Cetacea) of Drug Lahar in the Eastern Sulaiman range, Balochistan (Pakistan). Contributions from the Museum of Paleontology, University of Michigan, 30:269–319.

GINGERICH, P. D., M. UL-HAQ, L. S. ZALMOUT, I. H. KHAN, AND M. S. MALKANI. 2001b. Origin of whales from early artiodactyls: Hands and feet of Eocene Protocetidae from Pakistan. Science, 293:2239–2242.

HULBERT, R. C., JR. 1998. Postcranial osteology of the North American middle Eocene protocetid *Georgiacetus*, p. 235–267. *In* J. G. M. Thewissen (ed.), The Emergence of Whales, Evolutionary Patterns in the Origin of Cetacea. Plenum Press, New York, 477 pp.

HULBERT, R. C., JR., R. M. PETKEWICH, G. A. BISHOP, D. BURKY, AND D. P. ALESHIRE. 1998. A new middle Eocene protocetid whale (Mammalia: Cetacea: Archaeoceti) and associated biota from Georgia. Journal of Paleontology, 72:905–925.

KUMAR, K. AND A. SAHNI. 1986. *Remingtonocetus harudiensis*, new combination, a middle Eocene archaeocete (Mammalia, Cetacea) from Western Kutch, India. Journal of Vertebrate Paleontology, 6:326–349.

LUCAS, F. A. 1900. The pelvic girdle of Zeuglodon, *Basilosaurus cetoides* (Owen) with notes on other portions of the skeleton. Proceedings of the U.S. National Museum, 23:327–331.

LUCKETT, W. P. AND N. HONG. 1998. Phylogenetic relationships between the orders Artiodactyla and Cetacea: A combined assessment of morphological and molecular evidence. Journal of Mammalian Evolution, 5:127–182.

MADAR, S. I. 2007. The postcranial skeleton of early Eocene pakicetid cetaceans. Journal of Paleontology, 81:176–200.

MADAR, S. I., J. G. M. THEWISSEN, AND S. T. HUSSAIN. 2002. Additional holotype remains of *Ambulocetus natans* (Cetacea, Ambulocetidae) and their implications for locomotion in early whales. Journal of Vertebrate Paleontology, 22:405–422.

MUKHOPADHYAY, S. K. AND S. SHOME. 1996. Depositional environment and basin development during early Paleogene lignite deposition, western Kutch, Gujarat, India. Journal of the Geological Society of India, 47:579–592.

NUMMELA, S., S. T. HUSSAIN, AND J. G. M. THEWISSEN. 2006. Cranial anatomy of Pakicetidae (Cetacea, Mammalia). Journal of Vertebrate Paleontology, 26:746–759.

NUMMELA, S., J. G. M. THEWISSEN, S. BAJPAI, S. T. HUSSAIN, and K. KUMAR. 2004. Eocene evolution of whale hearing. Nature, 430:776–778.

NUMMELA, S., J. G. M. THEWISSEN, S. BAJPAI, S. T. HUSSAIN, AND K. KUMAR. 2007. Sound transmission in archaic and modern whales: Anatomical adaptations for underwater hearing. Anatomical Record, 290:716–733.

O'LEARY, M. A. 1998. Phylogenetic and morphometric reassessment of the dental evidence for a mesonychian and cetacean clade, p. 133–162. *In* J. G. M. Thewissen (ed.), The Emergence of Whales, Evolutionary Patterns in the Origin of Cetacea. Plenum Press, New York, 477 pp.

O'LEARY, M. A. AND J. GATESY. 2007. Impact of increased character sampling on the phylogeny of Cetartiodactyla (Mammalia): combined analysis including fossils. Cladistics, 23:1–46.

O'LEARY, M. A. AND J. H. GEISLER. 1999. The position of Cetacea within Mammalia: Phylogenetic analysis of morphological data from extinct and extant taxa. Systematic Biology, 48:455–490.

RAI, J. 1997. Scanning-electron microscopic studies of the late middle Eocene (Bartonian) calcareous nannofossils from the Kutch Basin, western India. Journal of the Palaeontological Society of India, 42:147–167.

SAHNI, A. AND V. P. MISHRA. 1972. A new species of *Protocetus* (Cetacea) from the middle Eocene of Kutch, western India. Palaeontology, 15:490–495.

SAHNI, A. AND V. P. MISHRA. 1975. Lower Tertiary vertebrates from Western India. Palaeontological Society of India, Monograph, 3: 1–48.

SARASWATI, P. K. AND R. K. BANARJEE. 1984. Lithostratigraphic classification of the Tertiary sequence of northwestern Kutch, p. 377–390. *In* R. M. Badve, V. D. Bokar, M. A. Ghare, and C. S. Rajshekhar (eds.), Proceedings of the Xth Indian Colloquium on Micropalaeontology and Stratigraphy, 1982, Pune. Marahastra Association for the Cultivation of Science, Pune.

SARAVANAN, N. 2007. Sequence-stratigraphy of vertebrate-bearing, early Tertiary strata of Gujarat, India. Unpubl. Ph.D. Thesis, Indian Institute of Technology, Roorkee, 215 pp.

SINGH, P. AND M. P. SINGH. 1991. Nannofloral biostratigraphy of the late middle Eocene strata of Kachchh Region, Gujarat State, India. Geoscience Journal (Dehra Dun, India), 12:17–51.

SWOFFORD, D. L. 2002. PAUP*: Phylogenetic Analysis Using Parsimony (and Other Methods) 4.0 Beta. CD-ROM, Sinauer, Sunderland, Connecticut.

THEWISSEN, J. G. M. 1994. Phylogenetic aspects of cetacean origins: A morphological perspective. Journal of Mammalian Evolution, 2:157–184.

THEWISSEN, J. G. M. AND S. BAJPAI. 2001a. Dental morphology of the Remingtonocetidae (Cetacea, Mammalia). Journal of Paleontology, 75:463–465.

THEWISSEN, J. G. M. AND S. BAJPAI. 2001b. Whale origins as posterchild for macroevolution. BioScience, 5:1037–1049.

THEWISSEN, J. G. M. AND F. E. FISH. 1997. Locomotor evolution in the earliest cetaceans: Functional model, modern analogues, and paleontological evidence. Paleobiology, 23:482–490.

THEWISSEN, J. G. M. AND S. T. HUSSAIN. 2000. *Attockicetus praecursor*, a new remingtonocetid cetacean from marine Eocene sediments in Pakistan. Journal of Mammalian Evolution, 7:133–146.

THEWISSEN, J. G. M. AND S. NUMMELA. 2007. Toward an integrative approach, p. 333–340. *In* J. G. M. Thewissen and S. Nummela (eds.),

Sensory Biology on the Threshold; Adaptations in Secondarily Aquatic Tetrapods. University of California Press, Berkeley, 360 pp.

THEWISSEN, J. G. M. AND E. M. WILLIAMS. 2002. The early evolution of Cetacea (whales, dolphins, and porpoises). Annual Review of Ecology and Systematics, 33:73–90.

THEWISSEN, J. G. M., L. J. ROE, J. R. O'NEIL, S. T. HUSSAIN, A. SAHNI, and S. BAJPAI. 1996. Evolution of cetacean osmoregulation. Nature, 381:379–380.

THEWISSEN, J. G. M., E. M. WILLIAMS, L. J. ROE, AND S. T. HUSSAIN. 2001. Skeletons of terrestrial cetaceans and the relationships of whales to artiodactyls. Nature, 413:277–281.

THEWISSEN, J. G. M., L. N. COOPER, M. T. CLEMENTZ, S. BAJPAI, AND B. N. TIWARI. 2007. Whales originated from aquatic artiodactyls in the Eocene Epoch of India. Nature, 450:1190–1194.

UHEN, M. D. 1998. Middle to late Eocene basilosaurines and dorudontines, p. 29–61. *In* J. G. M. Thewissen (ed.), The Emergence of Whales, evolutionary patterns in the origin of Cetacea. Plenum Press, New York, 477 pp.

UHEN, M. D. 2004. Form, function, and anatomy of *Dorudon atrox* (Mammalia, Cetacea): An archaeocete from the middle to late Eocene of Egypt. Museum of Paleontology, University of Michigan, Papers on Paleontology, 34:1–222.

ACCEPTED 17 APRIL 2009

APPENDIX 1

Material on which these analyses are based.

Andrewsiphius sloani (Sahni and Mishra, 1972)

IITR-SB 2871

2871.1	Cervical vertebra 6
2871.2	Cervical vertebra 7
2871.3	Caudal vertebra 9
2871.4	Thoracic vertebra 13
2871.5	Thoracic vertebra 9
2871.6	Cervical vertebra, centrum fragment
2871.7	Caudal vertebra 8
2871.8	Lumbar vertebra 8
2871.101	Vertebra, centrum fragment
2871.11	Caudal vertebra 19
2871.12	Caudal vertebra 18
2871.13	Sternum fragment
2871.14	Thoracic vertebra, spinous process
2871.15	Femur, left
2871.16	Caudal vertebra 10
2871.17	Humerus, right, distal part
2871.18	Humerus, left, distal part
2871.19	Mandible, left, fragment
2871.201	Humerus, right, proximal part
2871.21	Humerus, left, proximal part
2871.23	Mandible, left, fragment
2871.24	Premolar, fragment
2871.25	Lumbar vertebra 5
2871.26	Lumbar vertebra, centrum
2871.27	Canine or single-rooted premolar
2871.28	Caudal vertebra 14
2871.29	Patella
2871.301	Lumbar vertebra 3
2871.32	Phalanx, proximal, proximal part
2871.33	Squamosal fragment with mandibular fossa
2871.35	Tibia, right, proximal part
2871.36	Lumbar vertebra 4
2871.38	Thoracic vertebra 10
2871.39	Sacral vertebra 1, centrum
2871.401	Braincase
2871.41	Mandible, Fragment, left and right
2871.42	Mandibular condyle
2871.43	Occipital condyle
2871.44	Associated dentine and enamel fragments

Kutchicetus minimus Bajpai and Thewissen, 2000

IITR-SB 2647

2647.1	Thoracic vertebra 1
2647.2	Thoracic vertebra 2
2647.3	Cervical vertebra 6
2647.4	Thoracic vertebra 8
2647.5	Thoracic vertebra 9
2647.6	Thoracic vertebra 10
2647.7	Thoracic vertebra 11
2647.8	Thoracic vertebra 13
2647.9	Lumbar vertebra 1
2647.101	Lumbar vertebra 5
2647.11	Lumbar vertebra 6
2647.12	Lumbar vertebra 8
2647.13	Sacrum, fused sacral vertebrae 1–4
2647.14	Caudal vertebra 1
2647.15	Caudal vertebra 2
2647.16	Caudal vertebra 3
2647.17	Caudal vertebra 5
2647.18	Caudal vertebra 6
2647.19	Caudal vertebra 9
2647.201	Caudal vertebra 10
2647.21	Caudal vertebra 11
2647.22	Caudal vertebra 12
2647.23	Caudal vertebra 14
2647.24	Caudal vertebra 15
2647.25	Caudal vertebra 18
2647.26	Caudal vertebra 19
2647.27	Cervical vertebra, fragment
2647.28	Cervical vertebra, fragment
2647.29	Vertebral fragment
2647.301	Thoracic vertebra, fragment
2647.31	Atlas, fragment
2647.32	Ischium, fragment
2647.33	Iliac blade, fragment
2647.34	Pelvis, fragment
2647.35	Ilium, fragment
2647.36	Rib, proximal fragment

Kutchicetus minimus Bajpai and Thewissen, 2000

IITR-SB 2647

2647.37	Rib, shaft fragment
2647.38	Rib, proximal fragment
2647.39	Rostrum fragment with alveoli for C-P1
2647.401	Humerus, left, proximal part
2647.41	Femur, left, proximal part
2647.42	Humerus, left, distal part
2647.43	Tibia, right, proximal part
2647.44	Tibia, right, distal part
2647.45	Bone fragment
2647.46	Ilium fragment
2647.48	Skull fragment
2647.49	Bone fragment
2647.501	Femur, right, distal part
2647.51	Ulna, left, olecranon
2647.52	Radius, left, proximal
2647.53	Phalanx
2647.54	Femur, right, lateral condyle.
2647.55	Sesamoid
2647.56	Radius, right, proximal part
2647.57	Femur, left, greater trochanter
2647.58	Incisor, small, I1?
2647.61	Sternum fragment
2647.7	Cervical vertebra 4
2647.71	Cervical vertebra 5
2647.72	Thoracic vertebra 6
2647.73	Incisor, large I2–3?
2647.74	Canine, upper
2647.75	Molar, upper, fragment
2647.76	Premolar fragment
2647.77	Premolar fragment, P4?

APPENDIX 2

Phylogenetic scores for andrewsiphiines. A: Score for *Andrewsiphius*; K, score for *Kutchicetus*. Specimen numbers indicate one of the specimens on which this character can be scored, not all on which it can be observed. When no acronym is given, specimen is in the IITR-SB collection. Characters discussed by Geisler et al. (2005) and in text.

1. A: 1 (2517); K: 1 (2636)
2. A: 1 (2031, 2517, 2724); K: 1 (2791)
3. A: 2 (2907); K: unknown
4. A: 0 (2517); K: 0 (2791)
5. A: 0 (2517); K: 0 (2791)
6. A: 1 (2021); K: 1 (1007)
7. A: unknown; K: unknown
8. A: unknown; K: unknown
9. A: 2 (2021); K: 2 (2791)
10. A: 3 (2517); K: 3 (2791)
11. A: 3 (2517); K: 3 (2647)
12. A: 0 (2021); K: 0 (VPL 1007)
13. A: 1 (3153): K: 1 (VPL 1007)
14. A: 0 (2907); K: 0 (VPL 1007)
15. A: 2 (2907); K: unknown
16. A: 0 (3153); K: 0 (2791)
17. A: 1 (2907); K: 1 (2791)
18. A: 1 (3153); K: 1 (2791)
19. A: 0 (3153); K: 0 (2791)
20. A: 0 (3153); K: unknown
21. Uninformative character
22. Uninformative character
23. A: 2 (3153); K: unknown
24. A: 0 (3153); K: 0 (VPL 1007)
25. Uninformative character
26. A: 1 (2786); K: unknown
27. A: 0 (3153); K: 0 (VPL 1007)
28. A: 2, 3 (see discussion in text); K: 1 (1007)
29. A: 0 (2786); K: unknown
30. Uninformative character
31. A: 0 (3153); K: 0 (VPL 1007)
32. A: 0 (2907); K: unknown
33. Unknown
34. A: 0 (3153); K: 0 (VPL 1007)
35. Uninformative character
36. A: 1 (3153); K: 1 (VPL 1007)
37. A: 1 (3153); K: 1 (VPL 1007)
38. A: 0 (3153); K: 0 (VPL 1007)
39. Uninformative character
40. Uninformative character
41. A: 0 (2786); K: unknown

42. Uninformative character
43. Uninformative character
44. Uninformative character
45. A: 1 (2786); K: unknown
46. A: 1 (3153); K: unknown
47. A: 1 (2786); K: unknown
48. Uninformative character
49. A: 0 (3153 left and right bulla); K: unknown
50. A: 1 (3153); K: unknown
51. Uninformative character
52. A: 1 (3153); K: 1 (VPL 1007)
53. Uninformative character
54. A: 2 (3153); K: 2 (VPL 1007)
55. A: 0 (3153); K: 0 (VPL 1007); *Remingtonocetus*: 0 (2828)
56. A: 1 (3153); K: 1 (VPL 1007)
57. A: 3 (3153); K: 3 (VPL 1007)
58. A: 1 (3153); K: 1 (VPL 1007)
59. A: 0 (3153); K: unknown
60. A: 1 (3153); K: unknown
61. A: 0 (2786); K: unknown
62. A: 1 (3153); K: unknown
63. Uninformative character
64. A: 1 (3153); K: 1 (VPL 1007)
65. Uninformative character
66. A: 0 (2724); K: 0 (2636)
67. A: 1 (3153); K: 1 (2647)
68. A: 1 (LUVP 11060); K: 1 (2636)
69. A: 0 (2723); K: 0 (VPL 1007)
70. A: 1 (2723); K: 0 (2636)
71. A: 2 (2723); K: unknown
72. A: 0 (2723); K: unknown
73. A: 0 (2723); K: unknown
74. A: 0 (2723); K: 0 (2723)
75. A: 2 (3153); K: 2 (VPL 1007)
76. A: 3 (3153); K: 3 (VPL 1007)
77. A: F (3153: 2; 2907: 3); K: F (VPL 1007: 2; 2791: 3)
78. A: 1 (3153); K: 1 (VPL 1007)
79. A: F (3153: 2; 2907: 3); K: F (VPL 1007: 2; 2791: 3)
80. A: 4 (2723); K: 4 (2636)
81. A: 1 (2723); K:1 (2636); *Remingtonocetus*: 0 or 1 (IITR-SB 2704)
82. A: 1 (2723); K: 1 (2636)
83. A: 0 (2871); K: 0 (2647)
84. Unknown
85. A: unknown; K: 1 (2647)
86. Unknown
87. A: unknown; K: 0 (2647)
88. Unknown
89. A: unknown; K: 0 (2647)
90. Unknown
91. A: unknown; K: 2 (2647)
92. A: unknown; K: 1 (2647, as seen on S1)
93. A: unknown; K: 0 (2647)
94. A: unknown; K: 3 (2647)
95. A: unknown; K: 1 (2647)
96. Unknown
97. A: unknown; K: 0 (2647)
98. A: unknown; K: 0 (2647)
99. Unknown
100. Unknown
101. Unknown
102. Unknown
103. A: unknown; K: 0 (2647)
104. A: unknown; K: 0 (2647)
105. A: unknown; K: 1 (2647)
106. Unknown
107. A: unknown; K: 0 (2647)

APPENDIX 3—Scores (Sc.) for the new phylogenetic characters and the specimens on which they were based. Characters discussed in the text.

	108		109		110		111	
	Sc.	specimen	Sc.	specimen	Sc.	specimen	Sc.	specimen
Pakicetidae	0	H-GSP 1694	0	H-GSP 18410	0	H-GSP 18470	?	
Ambulocetus	1	H-GSP 18507	0	H-GSP 18507	0	H-GSP 18507	0	H-GSP 18507
Rodhocetus	?		0	GSP-UM 3012	?		0	Gingerich et al., 1994
Remingtonocetus	0	IITR-SB 2521	1	IITR-SB 2521	0	IITR-SB 2650	0	IITR-SB 2770
Dalanistes	?		?		?		?	
Gaviacetus	?		?		?		0	Gingerich et al., 1995
Carolinacetus	?		0	Geisler et al., 2005	?		?	
Protocetus	?		?		0	Kellogg, 1937	0	
Georgiacetus	0	Hulbert et al., 1998b	0	Hulbert et al., 1998b	0	Hulbert et al., 1998b	0	Hulbert et al., 1998b
Babiacetus	0	IITR-SB 2512	0	IITR-SB 2512	?		?	
Basilosaurus	0	Kellogg, 1936	1	Kellogg, 1936	0	Kellogg, 1936	0	Kellogg, 1936
Dorudon	0	Uhen, 2004	1	Uhen, 2004	0	Uhen, 2004	0	Uhen, 2004
Eocetus wardii	?		?		?		?	
E. schweinfurti	?		?		?		0	Stromer, 1903
Artiocetus	?		?		?		?	
Qaisracetus	?		?		?		?	
Andrewsiphius	1	IITR-SB 2723	0	IITR-SB 2723	1	IITR-SB 3153	1	IITR-SB 2751
Kutchicetus	1	IITR-SB 2636	?		?		1	VPL 1007

	112		113		114		115	
	Sc.	specimen	Sc.	specimen	Sc.	specimen	Sc.	specimen
Pakicetidae	0	H-GSP 96231	0	H-GSP 96254	0	H-GSP 96314	0	Madar, 2006
Ambulocetus	?		?		0	H-GSP 18507	1	H-GSP 18507
Rodhocetus	?		?		?		1	Buchholtz, 1998
Remingtonocetus	0	IITR-SB 2781	1	IITR-SB 2906	1	IITR-SB 2521	?	
Dalanistes	?		?		?		?	
Gaviacetus	0	Gingerich et al., 1995	?		?		?	
Carolinacetus	0	Geisler et al., 2005	?		1	Geisler et al., 2005	?	
Protocetus	0	Kellogg, 1936	?		?		?	
Georgiacetus	0	Hulbert et al, 1998b	?		1	Hulbert et al., 1998b	?	
Babiacetus	0	Gingerich et al., 1995	?		1	Gingerich et al., 1995	?	
Basilosaurus	0	Kellogg, 1936	1	Kellogg, 1936	0	Kellogg, 1936	1	Kellogg, 1936
Dorudon	0	Uhen, 2004	1	Uhen, 2004	1	Uhen, 2004	1	Uhen, 2004
Eocetus wardii	?		?		?		?	
E. schweinfurti	?		?		?		?	
Artiocetus	?		?		?		?	
Qaisracetus	?		?		?		?	
Andrewsiphius	1	IITR-SB 2786	?		1	IITR-SB 2723	2	IITR-SB 2786
Kutchicetus	1	VPL 1007	?		?		2	IITR-SB 2647